UNIVERSITA' VITA-SALUTE SAN RAFFAELE

CORSO DI DOTTORATO DI RICERCA INTERNAZIONALE IN MEDICINA MOLECOLARE

Curriculum in Experimental and Clinical Medicine

INVESTIGATING MOLECULAR AND IMMUNOLOGICAL MECHANISMS UNDERLYING HIV PERSISTENCE

DoS: Dott.ssa Silvia Nozza

Second Supervisor: Prof. Francesco Roberto Simonetti

Additional Supervisor: Dott.ssa Daniela Cesana

Tesi di DOTTORATO di RICERCA di Elena Bruzzesi

matr. 020255

Ciclo di dottorato XXXVII°

SSD MED/17

Silvia Nozza

Anno Accademico 2023/2024

CONSULTAZIONE TESI DI DOTTORATO DI RICERCA

La sottoscritta/*I* Elena Bruzzesi

Matricola / *registration number* 020255

nata a/ *born at* Modena (MO)

il/*on* 08/07/1991

autore della tesi di Dottorato di ricerca dal titolo / *author of the PhD Thesis titled*

INVESTIGATING MOLECULAR AND IMMUNOLOGICAL MECHANISMS UNDERLYING HIV PERSISTENCE

□ AUTORIZZA la Consultazione della tesi / AUTHORIZES *the public release of the thesis*

□ X NON AUTORIZZA la Consultazione della tesi per 9 mesi /DOES NOT AUTHORIZE *the public release of the thesis for ..... months*

a partire dalla data di conseguimento del titolo e precisamente */ from the PhD thesis date, specifically*

Dal / *from* 14/04/2025 Al / *To* 13/01/2026

Poiché /*because*:

X l'intera ricerca o parti di essa sono potenzialmente soggette a brevettabilità/ *The whole project or part of it might be subject to patentability;*

□ ci sono parti di tesi che sono già state sottoposte a un editore o sono in attesa di pubblicazione/ *Parts of the thesis have been or are being submitted to a publisher or are in press;*

□ la tesi è finanziata da enti esterni che vantano dei diritti su di esse e sulla loro pubblicazione/ *the thesis project is financed by external bodies that have rights over it and on its publication.*

E' fatto divieto di riprodurre, in Tutto o in parte, quanto in essa contenuto / *Copyright the contents of the thesis in whole or in part is forbidden*

Data /Date ...07/03/2025..... Firma /Signature .....

DECLARATION

This thesis has been:

- composed by myself and has not been used in any previous application for a degree. Throughout the text I use both 'I' and 'We' interchangeably.
- has been written according to the editing guidelines approved by the University.

Permission to use images and other material covered by copyright has been sought and obtained. For the following image/s (Figure 1.1), it was not possible to obtain permission and is/are therefore included in thesis under the "fair use" exception (Italian legislative Decree no. 68/2003).

All the results presented here were obtained by myself, except for:

1) *Characterization of putative predictive biomarkers: HLA class I- Killer-cell Immunoglobulin-like Receptor (KIR) matching (Results, chapter 4.2.2.) were performed by dr. Raniero Chimienti, Diabetes Research Institute (DRI), IRCCS San Raffaele Scientific Institute, Milan, Italy.*

All sources of information are acknowledged by means of reference. In particular, in paragraph 1.3.3.4 (pages 22-25) I will discuss the results of a previous publication I co-authored, which forms part of the study's rationale. The citation for this work is as follows: Cesana, D., et al., HIV-1-mediated insertional activation of STAT5B and BACH2 triggers viral reservoir formation in T regulatory cells. Nature Communications, 2017, 8, 498.

ABSTRACT

Main barrier to a sterilizing cure is the early establishment of a stable reservoir of HIV infected cells. Starting ART during acute infection supports immunological recovery, reduces the size of the HIV reservoir, and enhances the likelihood of post-treatment viral control. Several mechanisms contribute to maintenance of reservoir; the deregulation of BACH2 and STAT5B expression was shown to contribute to HIV persistence in regulatory T cells. On the other hand, myeloid cells have been described as reservoirs of HIV. We aimed to characterize acute and chronic HIV infection from an immunological perspective, describe the size and replication competence of the reservoir, and characterize the integration profile of HIV-1 in the context of the PERSHIST and in the IMMUNERaRe studies.

Adult people living with HIV (PLWH) treated either in chronic infection (CHI) with history of ART higher than 15 years or 5 years or in acute infection (AHI) were included in the PERSHSIT study, while in the IMMUNERaRe study only PWLH who started ART in AHI were included. Cytofluorimetric analysis was used to assess the relative composition of myeloid and lymphocytic cell subpopulations. Intact proviral DNA assay was used to quantify and distinguish deleted proviruses from intact proviruses. Chimeric transcripts were retrieved by RT-PCR, while integration sites by Sonicated Linker Mediated-PCR. Comparisons among groups were performed by nonparametric tests.

We enrolled 28 PLWH in PERSHIST study and 89 in IMMUNERaRe study. We found similar relative composition of conventional and non-conventional T-regulatory cells and of myeloid compartments with regulatory functions, also when compated to healthy controls. IPDA revealed a greater amount of intact DNA in PLWH who started ART in CHI (PERSHIST participants), as compared to AHI (IMMUNERaRe participants). BACH2 and, even more, STAT5B were confirmed to be culprit of integration. We identified specific HLA-KIR interactions associated with immunological control in PWH starting ART during PHI.

Our work enhances the understanding of the complex mechanisms underlying HIV persistence and immunological control in PLWH. The enrichment of activating KIR in RR suggests a role for NK cell-mediated responses in immune recovery.

ABSTRACT

La principale barriera a una cura sterilizzante è la precoce instaurazione di un serbatoio stabile di cellule infettate da HIV. L'inizio precoce della terapia antiretrovirale (ART) durante l'infezione acuta favorisce il recupero immunologico, riduce la dimensione del serbatoio virale e aumenta la probabilità di controllo virale post-trattamento. Diversi meccanismi contribuiscono al mantenimento del reservoir; la disregolazione dell'espressione di BACH2 e STAT5B è stata associata alla persistenza di HIV nelle cellule T regolatorie. D'altra parte, le cellule mieloidi sono state descritte come potenziali serbatoi dell'infezione. Gli obiettivi di questo studio erano caratterizzare l'infezione da HIV nelle fasi acute e croniche dal punto di vista immunologico, descrivere la dimensione e la competenza replicativa del reservoir, e caratterizzare i profili di integrazione di HIV-1 nell'ambito degli studi PERSHIST e IMMUNERaRe.

Lo studio PERSHIST ha incluso persone adulte con HIV (PLWH) trattate durante l'infezione cronica, con una storia di ART superiore a 15 anni o 5 anni o trattate in fase di infezione acuta. Nello studio IMMUNERaRe, invece, sono stati inclusi solo PLWH che avevano iniziato la ART durante l'AHI. L'analisi citofluorimetrica è stata utilizzata per valutare la composizione relativa delle sottopopolazioni linfocitarie e mieloidi specifiche. L'Intact Proviral DNA Assay è stato impiegato per quantificare e distinguere i provirus deleti da quelli intatti. I trascritti chimerici sono stati rilevati mediante RT-PCR, mentre i siti di integrazione sono stati analizzati tramite Sonicated Linker Mediated-PCR. Le comparazioni tra i gruppi sono state effettuate con test non parametrici.

Abbiamo arruolato 28 persone con HIV nello studio PERSHIST e 89 nello studio IMMUNERaRe. Abbiamo riscontrato una composizione relativa simile delle cellule T-regolatorie convenzionali e non convenzionali e delle compartimentazioni mieloidi con funzioni regolatorie, anche rispetto ai controlli sani. L'IPDA ha rivelato una maggiore quantità di DNA intatto nelle persone con HIV che hanno iniziato la ART in fase cronica (partecipanti a PERSHIST), rispetto a quelle in fase acuta (partecipanti a IMMUNERaRe). BACH2 e, ancora di più, STAT5B sono stati confermati come

responsabili dell'integrazione. Abbiamo identificato specifiche interazioni HLA-KIR associate al controllo immunologico in PWH che hanno iniziato ART durante la PHI.

Il nostro lavoro migliora la comprensione dei complessi meccanismi alla base della persistenza dell'HIV e del controllo immunologico in PLWH. L'arricchimento di KIR attivanti nei RR suggerisce un ruolo delle risposte mediate dalle cellule NK nel recupero immunologico.

THESIS OUTLINE

1. INTRODUCTION …...……..……..……7

1.1. HIV-1 infection …..…….…….……..7

1.1.1. Epidemiology of HIV infection ...……..7

1.1.2. Course of HIV disease …..…….9

1.2. Biology of HIV..…….……..……..……..…….……10

1.2.1. Viral structure……..…….……..……..11

1.2.2. Genome structure ……..……..11

1.2.3. HIV replication cycle ……...…12

1.3. HIV reservoir …….…...13

1.3.1. Reservoir: where? …….…….……..14

1.3.2. Reservoir: how to measure? ..……...……....15

1.3.3. Reservoir: how does it persist? ..……..16

1.3.3.1. Residual HIV replication …….16

1.3.3.2. Latency ……17

1.3.3.3. Proliferation of infected cells ……..…….……18

1.3.3.4. HIV integration …….……...20

1.3.3.4.1. Role of the genes BACH2 and STAT5B …….25

1.3.3.4.2. Regulatory T and myeloid compartment …….....26

2. AIM OF THE STUDY ……..……...32

3. MATERIALS AND METHODS …..…….....…….…33

3.1. PERSHIST study ……..…….……...……33

3.2. IMMUNERARE study ……..…….……..…....34

3.3. Lab methods……... ……..…….……..…….…….36

3.3.1. Cell purification and cytofluorimetric analysis ……...38

3.3.2. Intact proviral DNA assay ……...……...38

3.3.3. Sonicated Linker Mediated (SLiM)-PCR for identification of integration sites ……...……..39

3.3.4. Chimeric transcripts retrieval ……....……41
3.4. Statistical analysis ……...……..……42

4. RESULTS …..……...……...……42
4.1. PERSHIST study ……..42
4.1.1. Characteristics of the cohort ……. ……..42
4.1.2. Characterization of lymphocytic and myeloid regulatory cellular subpopulation …….……....45
4.1.3. Quantification of intact provirus …….…….50
4.1.4. Identification of the integration sites …….……..52
4.1.5. Identification of the chimeric transcripts …….…..……..55
4.2. IMMUNERARE STUDY …….55
4.2.1. Characteristics of the cohort ……. ……..55
4.2.2. Characterization of putative predictive biomarkers: HLA class I- Killer-cell Immunoglobulin-like Receptor (KIR) matching ……..…57
4.2.3. Quantification of intact provirus …….……60
4.3. Intact proviral HIV-1 DNA in acute and chronic HIV infection ……..61

5. DISCUSSION ……..……...…….61

6. CONCLUSION ……...……68

BIBLIOGRAPHY……..……..……...……...68

ACRONYMS AND ABBREVIATIONS

AHI	Acute HIV Infection
AIDS	Acquired Immunodeficiency Syndrome
aKIR	Activating KIR
ART	Antiretroviral Therapy
BM	Bone Marrow
cART	Combined Antiretroviral Therapy
CDC	Centers for Disease Control
CSF	Cerebrospinal Fluid
DAA	Direct-Acting Antiviral Agents
DC	Dendritic cells
ddPCR	Digital Droplet Polymerase Chain Reaction
DNA	Deoxyribonucleic Acid
ELISA	Enzyme-Linked Immunosorbent Assay
FDC	Follicular Dendritic Cells
HIV	Human Immunodeficiency Virus
HLA	Human Leukocyte Antigen
IN	Integrase
IC	Integration Site
ID	Patient Identifier
iKIR	Inhibitory KIR
IN	Integrase
IPDA	Intact Proviral DNA Assay
IS	Integration Site
iTregs	Induced Treg cells
KIR	Killer-cell Immunoglobulin-like Receptor
LTR	Long Terminal Repeat
MDR	Multi-Drug Resistant
MHC	Major histocompatibility complex
MRC	Myeloid regulatory cells
MSD	Major Splice Donor
nFGS	Near Full Genome Sequencing
PBMC	Peripheral blood mononuclear cells
PCR	Polymerase Chain Reaction
PLWH	People Living With HIV
PMN	Polymerphonuclear neutrophils
PTC	Post-treatment controllers
PR	Protease
PrEP	Pre-Exposure Prophylaxis
qPCR	Quantitative PCR
QVOA	Quantitative Viral Outgrowth Assay
RNA	Ribonucleic Acid
RT	Reverse Transcriptase
SIV	Simian Immunodeficiency Virus
STAT	Signal transducer and activator of transcription

Tcm	Central Memory T Cell
TCR	T Cell Receptor
Tem	Effector Memory T Cell
Teff	Effector T Cell
Tfh	Follicular T Helper Cell
Th	T helper
Treg	Regulatory T Cell
Tr1	Type 1 regulatory (Tr1) T cell
Tscm	Stem Central Memory T Cell
TSS	Transcription start site
UNAIDS	The Joint United Nations Programme on HIV/AIDS
WHO	World Health Organization

LIST OF FIGURES AND TABLES

Figure 1.1 Summary of the global and WHO regional HIV epidemic, 2023.

Figure 1.2. HIV-1 integration sites targeting *BACH2* (up) and *STAT5B* (down) found in PBMCs of 54 PLWH under cART.

Figure 1.3. Scheme of the RT-PCR strategy used to amplify chimeric HIV/*STAT5B* or HIV/*BACH2* transcripts.

Figure 3.1. Scheme of gating strategy for the selection of T CD4+ e T CD8+ cells.

Figure 3.2. Schematic of gating strategy for the selection of the cellular component of the myeloid cellular subtypes analyzed.

Figure 3.3. Illustration of ddPCR plot showing intact (Q2) and defective proviruses (Q1 and Q4) by IPDA.

Figure 3.4. Schematic of the SLiM-PCR.

Table 4.1. Participants' characteristics stratified for each group. ID: patient identifier. ART: antiretroviral therapy.

Table 4.2. Comparison of demographic and immune-virological characteristics among treatment groups.

Figure 4.1. Characterization of the lymphoid compartment.

Figure 4.2. Characterization of the memory CD4+ T cells lymphoid compartment.

Figure 4.3. Characterization of the memory CD8+ T cells lymphoid compartment.

Figure 4.4. Characterization of the regulatory lymphoid compartment.

Figure 4.5. Characterization of the regulatory myeloid compartment.

Figure 4.6. Characterization of the DC-10 compartment.

Table 4.3. Detection frequency for the chimeric transcripts HIV/*STAT5B* and HIV/*BACH2* per patients and among the three groups.

Figure 4.7. Quantification of intact and defective proviruses with deletion at 5' or at 3' in PERSHIST study.

Figure 4.8. HIV-1 integration profile in the 13 enrolled subjects.

Figure 4.9. HIV-1 integration sites absolute (a) and relative (b) abundance.

Figure 4.10. HIV-1 integration sites distribution withing genes (A) and by transcriptional orientation among 265 genes hit at least twice with the same IS (B).

Table 4.4. Overall participants' characteristics stratified for each group.

Figure 4.11. Proportion of PLWH with the protective haplotypes containing high-expression HLA-C2 alleles, with and without HLA-B Bw4-Isoleucine8 (I8), among the three groups.
Figure 4.12. Proportion of PLWH with matches and mismatches of functional pairs between protective alleles and their activating KIR counterparts.
Figure 4.13. Proportion of PLWH with activating (aKIR) and inhibitory (iKIR) KIR within each group.
Figure 4.14. Quantification of intact and defective proviruses with deletion at 5' or at 3' in IMMUNERaRe study.
Figure 4.15. Quantification of intact and defective proviruses with deletion at 5' or at 3' in PERSHIST study who started ART in CHI (N=16) and PLWH enrolled in IMMUNERaRe study who started ART in AHI (N=86).
Figure 5.1. Schematic representation of the Chim-seq strategy to be employed to retrieve chimeric transcripts, specifically amplifying those originating between the integrated HIV genome and the surrounding cellular gene.

1. INTRODUCTION

1.1. HIV-1 infection

HIV-1 is the virus that causes acquired immunodeficiency syndrome (AIDS), recognized as one of the most catastrophic viral pandemics in history. The epidemic began in 1981, when the first case of AIDS was reported in a man who has sex with man in the USA. HIV was first identified and associated in 1983 [1, 2].

1.1.1. Epidemiology of HIV infection

HIV infection is a significant global public health concern. By the close of 2023, around 39.9 million individuals were living with HIV, with 65% of them located in the WHO African Region. During that year, it is estimated that 630,000 people died from HIV-related illnesses, and approximately 1.3 million new infections occurred. Most of these cases are found in Sub-Saharan Africa, which accounts for two-thirds of all new HIV infections worldwide, according to the World Health Organization (WHO).

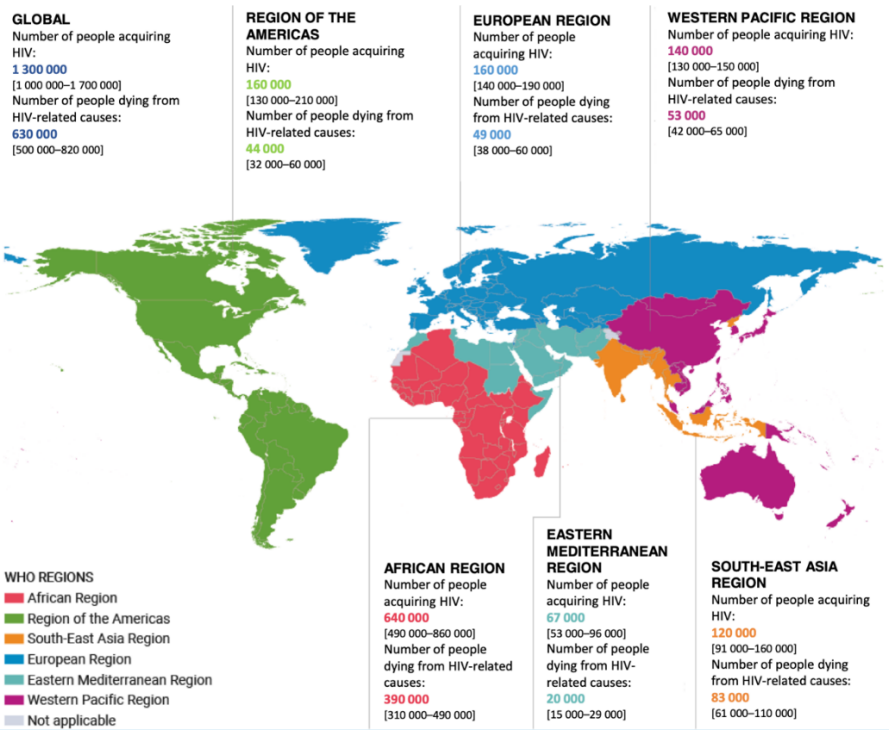


Figure 1.1. Summary of the global and WHO regional HIV epidemic, 2023.

UNAIDS have put forward the “95-95-95” strategy, setting the targets to be reached by 2030 to reduce AIDS-related deaths, calling for:

- 95% of HIV-infected individuals to be diagnosed by 2030
- 95% of whom will be on anti-retroviral therapy (ART)
- 95% of whom will achieve sustained virologic suppression.

In 2023, 86% of individuals living with HIV (PLWH) were aware of their HIV status. Among those who knew their status, 77% were receiving treatment, and of those on treatment, 72% achieved viral suppression. However, significant barriers to the global eradication of HIV remain, particularly in terms of limited access to HIV testing services and antiretroviral therapy (ART) coverage. In response to these challenges, In July 2016, the WHO introduced consolidated guidelines that removed all eligibility restrictions for HIV therapy, ensuring access to treatment for everyone living with HIV [3].

Globally, HIV is classified as HIV-1 and HIV-2, based on genome organization and phylogenetic relationships with other primate lentiviruses. HIV-1 is the most widespread type, while HIV-2 accounts for only 5% of infections, primarily found in West Africa. Notably, HIV-2 typically has a slower progression than HIV-1 but is less responsive to some ART classes, such as NNRTI[4]. Additionally, HIV-1 is divided into three distinct virus groups—M, N, O, and P—where the M group is the most prevalent and includes 10 subtypes [5].

At present, there is no known cure for HIV; however, antiretroviral therapies can control viral replication, decreasing the amount of circulating virus. In 1997, it became feasible for the first time to reduce plasma HIV-1 levels below the detection limit of clinical tests through the use of a combination of three antiretroviral medications [6]. This method, known as highly active antiretroviral therapy (HAART) or combined antiretroviral therapies (cART), significantly reduced mortality from HIV-1 infection. The advent of cART has transformed HIV from a deadly disease into a manageable chronic condition: mortality rates is decreased as a result of the prevention of both AIDS-related and non-AIDS-related complications.

Although cART represents a significant advancement, antiretroviral therapies do not provide a cure, due to the existence of a viral reservoir. Indeed, after ART is stopped, the virus rebounds in a median of three weeks. To achieve a definitive cure for HIV-1, which is defined as the ability to control viral replication without ART, three primary strategies

should be explored: an eradication approach that seeks to eliminate all viral reservoirs; a functional cure that focuses on managing viral replication without eradicating the reservoirs; and a hybrid cure that aims to reduce the reservoirs by enhancing immune responses [7]. Currently, there are only six anecdotal cases of successful eradication following stem cell transplants. The first of these was the Berlin patient [8], who received a transplant in 2009 from a donor homozygous for CCR5 delta32. Other notable cases include the 'London patient', 'Düsseldorf patient, 'woman from New York City, 'City of Hope patient,' and the 'Geneva patient,' all of whom underwent similar procedures [9,10,11,12]. Nevertheless, additional research is needed to better understand the mechanisms behind viral persistence.

1.1.2. Course of HIV disease

The defining characteristic of HIV infection is a severe immunodeficiency primarily due to CD4 T cells depletion. T helper cells are identified by the presence of the CD4 molecule, which serves as the receptor for HIV. The progression of HIV infection can be divided into several stages: viral transmission, acute HIV infection (AHI), seroconversion, and chronic HIV infection. The chronic phase may be clinically latent or symptomatic, eventually leading to acquired immunodeficiency syndrome (AIDS). After HIV transmission, the virus primarily infects macrophages, resident CD4+ T cells, dendritic cells (DC), and especially Langerhans cells (LC) to penetrate the epithelial barrier of mucosal surfaces [13]. The virus then rapidly migrates to the draining lymph nodes, which poses a challenge to the effectiveness of post-exposure vaccines [14]. Ultimately, upon infection, CD4+ T cells disseminate the virus through the bloodstream to other lymphoid tissues. The primary targets of HIV include T-cells, macrophages, and possibly dendritic cells, depending on the viral tropism. The chemokine receptor CCR5 is the main co-receptor utilized, although variants that use the CXCR4 co-receptor can emerge during the infection. Specifically, R5 viruses can infect both lymphocytes and macrophages, while X4 isolates are limited to T-cell lines. The decline in CD4+ T cells is rapid, significant, and irreversible from the early stages of infection [15]. This phase is referred as AHI or primary HIV infection and is marked by high amount of HIV-RNA and a temporary decrease in CD4+ T cell count. This initial infection with HIV-1 is often associated with an acute mononucleosis-like clinical syndrome that typically appears a few weeks after infection. However, many individuals in the early stages of HIV infection

remain asymptomatic. The dynamics of HIV viremia and antibody seroconversion can be categorized using the Fiebig classification, which includes six stages [16]. Those who begin antiretroviral therapy (ART) within six months of infection are more likely to become post-treatment controllers (PTCs), demonstrating viral control without ART after an initial suppression period. Notably, most PTCs do not possess protective HLA B alleles that are commonly found in spontaneous HIV controllers and instead carry risk-associated HLA alleles that are largely absent in these controllers[17]. Approximately three to six weeks post-infection, both cellular and humoral immune responses begin, leading to a reduction in viremia and antigen levels, CD4+ T cell counts stabilize, and clinical syndrome resolves. Within about six months, viremia stabilizes reaches its zenith, which, along with the nadir of CD4+ T cells, is used as a predictor of disease progression [18]. During the chronic phase of the disease, HIV continues to replicate in asymptomatic patients who are not on ART, eliminating approximately10 billion CD4 cells every day [19]. Conversely, ART effectively inhibits HIV replication, reducing plasma HIV-1 RNA levels below the detection limits of commercially available assays. Consequently, ART that achieves sustained viral suppression enhances immune function, improves overall quality of life, reduces the risk of both AIDS-defining and non-AIDS-defining complications, and extends lifespan.
Importantly, HIV infection is distinct among human viral infections because the virus evades the immune response while paradoxically triggering immune activation, which helps it persist in the host. This reservoir of the virus represents a significant barrier to achieving eradication of the infection.

1.2. Biology of HIV

HIV belongs to the *Lentivirus* genus, a subgroup within the *Retroviridae* family. Other members of this genus include the simian immunodeficiency virus (SIV). Like all retroviruses, HIV possesses an RNA genome that undergoes reverse transcription upon entering a new host cell. This process is mediated by the viral enzyme reverse transcriptase (RT), which converts the RNA genome into a complementary DNA (cDNA) copy. Initially, this results in an RNA-DNA hybrid, which is subsequently transformed into double-stranded DNA. The resulting DNA, known as the *provirus*, integrates into

the host cell's genome, in contrast to the classical pathway of genetic information flow from DNA to RNA and then to proteins.

1.1.1. Viral Structure

HIV is a spherical, enveloped RNA virus with a diameter of approximately 120 nm. It features a distinct three-layered composition, that comprehend an inner core containing the viral genome, a middle nucleocapsid, nn outer lipid-protein envelope.

The envelope, acquired through budding from the host cell membrane, consists of lipoproteins derived from the host, along with viral glycoproteins. The viral membrane contains heterodimeric glycoprotein complexes arranged as trimers, comprising surface-exposed spikes (gp120, or SU) and transmembrane anchoring pedicles (gp41, or TM), which are bound together. Gp120 facilitates viral entry by interacting with host cell surface receptors, dictating tissue tropism, while gp41 aids in membrane fusion.

Encased within the envelope is a capsid, composed of Matrix protein (MA or p17), Capsid protein (CA or p24), Nucleocapsid protein (NC or p7). The capsid also houses three key viral enzymes: Protease (PR), Reverse transcriptase (RT), Integrase (IN).

Additionally, the virus carries accessory proteins such as Nef, Vif, and Vpr, which play roles in immune evasion and viral replication.

1.1.2. Genome Structure

The HIV genome consists of two identical single-stranded RNA molecules, with a length of approximately 7 to 11 kilobases. It contains three primary genes essential for viral structure and function, common to all retroviruses. First, the Gag gene encodes core structural proteins, including p24 (capsid), p7 and p6 (nucleocapsid), and p17 (matrix). The Env gene encodes the envelope glycoproteins gp120 and gp41.

The Pol gene encodes key viral enzymes, including RT, IN (which integrates the provirus into the host genome), and PR (which processes precursor proteins into functional components). In addition to these core genes, HIV-1 possesses unique proteins, namely accessory proteins (Vif, Vpr, Vpu, and Nef) and regulatory proteins (Tat and Rev). At both genome termini, HIV contains Long Terminal Repeats (LTRs), which include promoter and enhancer regions crucial for transcriptional regulation. These sequences

interact with host cell transcription factors, influencing viral gene expression and replication [20].

1.1.3. HIV Replication Cycle

The HIV replication cycle follows six key steps: (1) binding and entry, (2) uncoating, (3) reverse transcription, (4) provirus integration, (5) virus protein synthesis and assembly, and (6) budding.

During the integration phase, the HIV genome undergoes reverse transcription after being released into the cytoplasm. Reverse transcriptase (RT) plays a crucial role in this process by using the tRNA present in the virion as a primer to synthesize a complementary negative-strand DNA, known as cDNA. Through its ribonuclease H active site, RT initiates synthesis at the primer binding site and continues until the viral RNA is fully transcribed into an RNA/DNA hybrid double helix. As the process progresses, RT degrades the original RNA genome while the polymerase function generates a positive-strand DNA, forming a double-helix DNA molecule. The fidelity of reverse transcription is influenced by the cellular protein APOBEC3G, and given its critical role, RT is a primary target for antiretroviral drugs.
Once synthesized, the viral DNA is transported into the nucleus as part of a pre-integration complex, a process directed by the accessory protein Vpr. Not all newly synthesized viral DNA molecules integrate into the host genome; some remain as circular molecules containing one or both long terminal repeats (LTRs). These unintegrated forms of DNA, including linear, 1-LTR, or 2-LTR circles, result from cellular ligase activity. Through the catalytic function of integrase (IN), the viral DNA is covalently inserted into the host genome. This occurs by cleaving nucleotides at the 3' ends of the double-stranded DNA, generating sticky ends that facilitate integration.

Integration is a critical step for the stable maintenance of the viral genome and is essential for viral replication. While integration site selection in the host genome is relatively nonspecific, HIV exhibits preferences both in vitro and in vivo. Studies have shown that HIV favors integration into highly expressed genes located in gene-dense regions without a clear preference for transcriptional orientation in in vitro conditions. However, in in

vivo settings, particularly in the pre-antiretroviral therapy (pre-ART) phase, integration often occurs in an orientation opposite to that of the host gene [21-25].

HIV also shows a tendency to integrate at specific sequences, depending on where the IN enzyme binds and cuts the host DNA. Sequences such as 5′-AAT, 5′-TAA, and 5′-AAA are enriched at integration sites. Despite these preferences, no definitive integration "hot spots" have been identified [26, 27].

Once integrated into the host genome, the HIV-1 provirus serves as a template for transcription. In the early stages of infection, HIV-1 initially produces only short, completely spliced mRNAs that encode the viral regulatory proteins Tat and Rev. Transcription from the HIV genome is controlled by the 5′ LTR viral promoter and regulated by specific viral proteins, particularly Tat and Rev, which play key roles in enhancing viral gene expression and replication.

1.3. HIV reservoir

The HIV-1 reservoir has been defined by Eisele and Siliciano as a population of infected cells that enables the persistence of replication-competent HIV in patients on optimal cART over a period of years [28]. Its maintenance represents the most significant obstacle to HIV eradication, as current therapies only block HIV replication but do not eliminate the virus.

The formation of the reservoir is an early event in infection. Chun et al. demonstrated that initiating cART as early as 10 days after the onset of primary HIV-1 symptoms did not prevent the establishment of the reservoir [29]. In fact, the HIV DNA set-point is established early during acute HIV infection [30].

The importance of the reservoir has been emphasized by treatment interruption studies, which showed that viremia rebounded after cART discontinuation, proving that even lifelong ART is insufficient for eradication. Specifically, in PLWH suppressed on ART for more than 7 years, the reservoir decays slowly, with a half-life of 44 months. Computational analyses suggest that eradication would required more than 60 years of ART, highlighting the urgent need for alternative therapeutic strategies [31]. Although they make up a small proportion of the reservoir, infected cells harboring an intact provirus are critical to the persistence of the virus. It was once believed that proliferating

CD4+ T-cell could not have a replication-competent HIV-1 virus, as viral protein expression would be cytotoxic. However, it is now understood that only a small fraction (11.3%) of integrated proviruses are intact [32]. Intact proviruses are responsible for the resurgence of viremia upon ART discontinuation. They can persist in cells in a reversible state of latency, actively silencing viral transcription, or reside in cell clones that undergo proliferation upon certain stimuli, as will be discussed later in this chapter.

1.3.1. Reservoir: where?

The largest reservoir of latently infected cells is found in the CD4+ T cell compartment, with resting CD4 T cells identified as the primary cellular reservoir. These cells are categorized based on their differentiation and memory status into naive T cells, central memory T cells (Tcm), transitional memory T cells (Ttm), and effector memory T cells (Tem). Tcm cells (CD45RA− CCR7+ CD27+) are long-lived, with a low proliferation rate and self-renewing capabilities; they reside in lymph nodes due to their expression of the chemokine receptor CCR7. When stimulated by antigens, Tcm cells proliferate and differentiate into Ttm cells (CD45RA− CCR7− CD27+), which replicate at a low but continuous rate. Ttm cells then differentiate into Tem cells (CD45RA− CCR7− CD27−), a highly proliferative population involved in T cell homeostasis, contributing minimally to the reservoir pool [33]. Additionally, other subsets of T cells, including Th1, Th2, Th17, Treg, and follicular T helper (Tfh) cells, have been suggested as reservoirs, with Treg and Tfh cells playing a central role as cellular reservoirs in lymphoid tissues.

T-memory stem cells (CD45RA+ CCR7+ CD27−) have also been proposed as a key reservoir, offering a privileged site for long-term viral persistence due to their stable and self-renewing properties [34].

In the myeloid compartment, macrophages are long-lived cells that promote HIV persistence, particularly in the spleen, gut, lungs, and CNS, owing to their intrinsic resistance to the cytopathic effects of HIV, which allows for low-level replication[35]. Similarly, microglial cells and astrocytes, with their low turnover, are permissive to HIV infection [36]. Furthermore, dendritic cells (DCs) in lymphoid tissues can internalize HIV, storing it in early endosomal systems without degrading it. HIV present on the surface can remain infectious for several days and can be transmitted to CD4+ T cells [37]. Follicular dendritic cells (FDCs) in lymph nodes germinal centers are particularly adept at trapping a significant amount of both infectious and defective extracellular

virions, making them the major source of HIVRNA, both in the pre-symptomatic and in the late stages of the infection [38].

1.3.2. Reservoir: how to measure the reservoir?

Despite years of extensive research, an optimal technique to accurately determine and monitor the size of the HIV reservoir has not yet been identified, primarily due to technical challenges. An ideal method would need to be sensitive enough to detect rare infected cell clones in a large background of uninfected cells and specific enough to differentiate between replication-competent and replication-incompetent proviruses. This is particularly urgent in the context of cure strategies.

Currently, the primary methods used to quantify the reservoir are based on culture assays and PCR-based measurements. PCR-based assays are the most sensitive, fastest, and easiest to use for detecting the prevalence of HIV-infected cells, as they quantify total, integrated, and unintegrated HIV DNA. The most used method to quantify HIV DNA is real-time PCR (qPCR) [39], but since qPCR exponentially amplifies noise at low copy numbers, which can reduce accuracy, droplet digital PCR (ddPCR) has been put forward as a potential alternative [40]. Total HIV-DNA PCR measurements can also identify unintegrated DNA forms, including 1-LTR and 2-LTR circles, which arise from unsuccessful integration. While these forms are part of the latent reservoir, 2-LTR circles were utilized as indicators of recent infection [41]. PCR-based HIV-DNA assays do not differentiate between defective and intact proviral genomes, particularly when amplifying a single sub-genomic region such as gag, which can lead to an overestimation of the reservoir size. In contrast, near full genome sequencing (nFGS) has revealed that the majority of proviruses in individuals on treatment are defective, due to substantial internal deletions, mutations in critical regulatory regions like the major splice donor (MSD) and packaging signal (ψ), and APOBEC3G-driven G-to-A hypermutation. A recent study discovered that nFGS methods do not offer an accurate quantitative assessment of intact proviruses, as only approximately 30% of intact proviruses were detected, while proviruses with significant internal deletions were amplified at expected frequencies [42]. Terminal-dilution co-culture assays, designed to detect replication-competent virus, can efficiently identify one infectious unit among hundreds of HIV proviral genomes. The quantitative viral outgrowth assay (QVOA) is the method most widely used for this

purpose, but it tends to underestimate the size of the latent reservoir [43]. Moreover, QVOA requires significant resources in terms of materials, labor, and costs, making it impractical for routine clinical use.

A more recent approach, the intact proviral DNA assay (IPDA), has been introduced as a method for measuring the HIV reservoir. Unlike long-distance PCR, IPDA can distinguish between intact and defective proviruses. It utilizes multiplexed droplet digital PCR (ddPCR), enabling the quantification of single template copies through short, highly efficient PCR reactions with digital calculation of input template molecules [44, 45]. ddPCR assay employs duplex PCR to target two regions: the ψ/MSD site and the Rev-response element in the env gene. There sites are frequently deleted or hypermutated in defective proviruses. On the other hand, when amplification occurs in both regions, the provirus is intact [42, 45].

Additionally, assays measuring viral protein expression induction, such as the ultrasensitive digital ELISA platform for quantifying HIV-1 p24 protein, have been explored for assessing viral production at the single-cell level. However, defective proviruses can also produce viral proteins, which may complicate interpretation [46]. The intact provirus detected by IPDA has been shown to correlate with total and integrated HIV levels [47].

1.3.3. 1.3.3. Reservoir: how does it persist?

HIV persistence is maintained by continuous cycles of HIV replication in specific anatomical sanctuaries, resulting in the infection of new cells. Other mechanisms are viral latency and the proliferation of infected clones.

1.3.3.1. Residual HIV replication

Low-level HIV replication predominantly takes place in areas defined as anatomical sanctuaries. They are characterized by concentration of cells permissive to infection, suboptimal ART penetration, and a pro-inflammatory milieu. These sites include primary and secondary lymphoid organs, the gastrointestinal (GI) tract, the central nervous system, and the genitalia.

Immune hyperactivation, a condition of widespread immune activation induced by inflammation, microbial translocation and co-infections, can also contribute to viral replication.

On the other hand, studies of ART intensification, which involve adding an antiretroviral drug (e.g. raltegravir) to the standard three-drug regimen, have shown no significant effect on plasma viremia. This indicates that replication is probably not the primary factor responsible for HIV persistence [48]. Moreover, the lack of viral phylogenetic evolution, the absence of mutations conferring drug resistance, and the identification of identical viral sequences even after extended ART further suggest that continuous viral production is not a key factor in sustaining HIV persistence [49].

1.3.3.2. Latency

In HIV infection, latency refers to the provirus integrating into the host cell genome in a way that is reversible and non-productive. While this integration typically does not lead to active viral replication, there have been rare instances where productive integration has been observed [50]. This process results in reversible silencing, allowing the virus to persist over time. While transcriptional silencing plays a central role in establishing latency, post-transcriptional mechanisms, such as the inhibition of nuclear RNA export and the suppression of HIV-1 translation by microRNAs, also contribute to maintaining this state. Furthermore, latency can be established even before genomic integration occurs [51].

Latency is both an early and a rare event. In PLWH undergoing long-term combination, latently infected cells show low frequency, ranging from 0.1 to 10 infectious units/million resting CD4+ T cells [52]. Notably, an even smaller subset of these cells contains an integrated provirus that retains the ability to replicate [28]. Resting CD4+ T cells serve as the primary cellular reservoir due to their long half-life and reduced permissiveness to viral replication. While most infected CD4+ T cells die, a small fraction survives and transitions into a resting state; they persist as memory cells [53].

The length of the latent phase is primarily governed by the lifespan of infected cells and their descendants. Nonetheless, latently-infected cells can be reactivated by homeostatic or antigenic stimuli, leading to the activation of proviral transcription and the release of new viruses.

1.3.3.3. Proliferation of infected cells

In individuals with HIV undergoing long-term antiretroviral therapy (ART), a substantial proportion of infected cells expand clonally, as evidenced by the identical integration sites of their proviruses [54, 24]. Integration site analysis is used to identify these HIV-1 clones and to track them over time, revealing that many infected CD4+ T cells in individuals on prolonged, effective ART harbor proviruses integrated at the same genomic location. This pattern is not random, as HIV replication is highly efficient yet error-prone [22, 55], leading to the continuous accumulation of new viral variants. In chronically infected individuals who are not on ART, the average pairwise nucleotide divergence between HIV variants ranges from 1.5% to 2%, meaning that no two viral genomes in the plasma are identical [56]. Given the relatively nonspecific nature of HIV-1 integration, the proliferation of infected cells could originate either from a genetically homogeneous initial population of infected cells or from the expansion of cells harboring proviruses integrated at the same site [22]. Initially, it was believed that only cells carrying defective proviruses could undergo clonal expansion [57]. However, Simonetti et al. (2016) identified a highly expanded clone of HIV-infected CD4 T cells harbouring a replication-competent provirus, known as AMBI-1. This clone could produce infectious virus and sustaining persistent plasma viremia despite ongoing ART in a patient with squamous cell carcinoma [48].

HIV clones originate during the pre-ART phase [58] and can persist for years. Notably, these clones have been shown to continue replicating under ART and remain detectable even during viral rebound within weeks of ART discontinuation [24, 54, 59]. The clonal expansion of HIV-1-infected cells provides an explanation for clinical phenomena such as viral blips or low-level viremia, which occur despite effective ART. Intermittent low-level viremia, defined as transient episodes of plasma viral loads below 200 copies/ml, does not involve the emergence of drug resistance mutations and does not respond to treatment intensification. Consequently, these fluctuations do not necessitate changes in ART regimens. Phylogenetic analysis of viral sequences during episodes of low-level viremia has shown that these transient increases in viral load are driven by genetically identical viruses, referred to as predominant plasma clones [55, 48, 60].

Several factors contribute to the clonal expansion of infected cells, including antigen-driven proliferation, homeostatic proliferation and integration site-driven proliferation. Homeostatic proliferation is regulated by cytokines such as IL-7 and IL-15, which help maintain the pool of memory CD4 T cells, particularly central memory (Tcm) and transitional memory (Ttm) cells. This process allows infected cells to persist without triggering viral gene expression, thereby evading immune clearance. Notably, IL-7 levels have been found to correlate inversely with reductions in the HIV reservoir, with previous studies linking IL-7 to plasma levels and CD4 T cell depletion. IL-7 facilitates the survival of infected CD4 T cells, supporting both the quantitative and qualitative stability of the viral reservoir [61, 62].

The expansion of memory CD4 T cells can also be triggered by antigenic stimulation, which includes the recognition of self or of foreign peptides presented by MHC class II molecules [63]. Antigen stimulation likely activates antigen-specific HIV-infected CD4 T cells, promoting both viral gene expression and clonal expansion. As a result, the prevalence of predominant plasma clones increases during peaks of antigenic stimulation and decreases as the corresponding immune response wanes over time [64]. This dynamic leads to viral blips and, in some cases, prolonged periods of stable or intermittent viral production with a median duration of 3.2 years [65]. The extent of HIV-1-infected cell expansion depends on the nature of the antigen involved. Antigen-presenting cells can provide continuous stimulation to HIV-1-specific CD4+ T cells, driving their proliferation. However, CD4 T cells specific for tuberculosis (TB) or Candida are often infected and depleted during HIV-1 infection [66, 67]. In contrast, cytomegalovirus (CMV)-specific CD4 T cells remain relatively preserved, maintaining both functionality and abundance. These cells may proliferate at higher rates due to recurrent CMV antigen stimulation and their sustained capacity for expansion [68, 69].

While these immune-driven mechanisms regulate HIV-1 clonal expansion under normal physiological conditions, HIV-1 integration can also induce aberrant cellular proliferation independent of immune system control. The identification of identical integration sites during ART provides evidence that certain infected cells can undergo sustained proliferation despite harboring an integrated virus. These integration events are often found in genes associated with cell survival and proliferation, suggesting that viral integration itself can drive expansion by altering host gene expression [24, 54].

Unlike antigen- or cytokine-driven expansion, HIV-1 integration site-driven clonal expansion progresses at a slower but continuous rate, contributing to the long-term persistence of infected cells.

1.3.3.4. HIV integration

Integration of HIV-1 viral genome is a relatively random event, as the virus exhibits certain site preferences, usually determined by the interaction between HIV integrase and host DNA [22]. Although retroviruses exhibit considerable variation, each has a weak consensus sequence at its integration site (>20 nucleotides), with a palindromic structure due to integrations occurring in both directions [22]. HIV shows a preference for integrating into intragenic regions of actively transcribed genes, with nearly 80% of integration events occurring within genes, including both exons and introns [70]. Additionally, HIV often integrates into specific sequences, such as 5′-AAT, 5′-TAA, and 5′-AAA [26].

Once integrated, the provirus becomes a permanent part of the host cell genome. As an infected cell replicates, all of its progeny will carry the provirus integrated at the same site as the parent cell. Therefore, integration sites can be used to trace the clonal expansion of an infected cell. When the integration sites of exogenous retroviruses are in or near proto-oncogenes, then they become oncogenic by exploiting the mechanism of insertional mutagenesis [71].

Insertional mutagenesis is the process by which an exogenous DNA sequence integrates within the genome of a host organism, resulting in the deregulation of part or all genes in the proximity of the insertion site. Retroviral insertion can interfere with the expression of host genes to promote cancer formation by means of four mechanisms, namely promoter insertion, enhancer activation, protein fusion and transcript stabilization.

Promoter insertion occurs when the insertion of the provirus falls into an endogenous promoter in the same transcriptional orientation as the target cellular gene; hence, the expression of the targete gene is increased, being under the control of the viral promoter, which are very active. Specifically, both 5’ and 3’ LTR can initiate the transcription, but the 5’ always generates fusion transcripts carrying both viral and cellular sequences. Also, the 3’ promoter can activate transcription, but only when the insertion results in the deletion of the 5’ LTR, a phenomenon known as promoter occlusion [72].

Then, transcriptional enhancement is the most frequent oncogenic mechanism, encompassing proviral enhancer insertion either at the 5' end or at the 3', in the opposite or in the same transcriptional orientation, respectively. When the provirus integrates nearby or within the host gene, host gene expression is increased host gene expression, being under the control the endogenous promoter and the proviral enhancer sequences as viral enhancers increase the activity of the promoter of the targeted gene with transcription starting at the normal transcription start site (TSS) [58].

Finally, the integration can occur via intragenic insertion, resulting into protein truncation. When the provirus integrates into the 3' UTR of a gene, it can result in loss of mRNA-destabilizing sequences and in the degradation of the transcript. The loss of this control results in the upregulation of the gene, generating an increased number of truncated but wild-type protein-encoding mRNA [73].

In animals, oncoretroviruses were found to activate proto-oncogenes leading to cancer by insertional mutagenesis mechanisms [74]. Moreover, HIV-1-derived lentiviral vector were found to interfere with the transcription of the targeted genes in hematopoietic cells, leading to their activation or inactivation and usually inducing aberrantly spliced viral/cellular chimeric mRNAs. On the contrary, it was thought that HIV-1 could not exploit insertional activation mechanisms because of the cytopathic effects of infection in transformed cells. However, an enrichment of HIV-1 integrations in cancer-associated genes, such as *BACH2* and *MLK2*, consistent with the rules of insertional activation was described in patients under cART [24, 54], suggesting that insertional mutagenesis mechanisms could promote the persistence of HIV-1 in the infected hosts. In depth, Ikeda et al. found an accumulation of viral integration in the BACH2 gene in 7 out of 7 HIV-infected subjects on suppressive antiretroviral treatment, and in the intron 1 of the STAT5B gene in 4 out of the 7 patients; all integrations were found to be in the same orientation as the targeted gene [75]. They also demonstrated that these integrations were maintained at different time points, indicating that cells carrying HIV-1 gene integrated at this locus were maintained during ART. The results were later confirmed by Maldarelli et al. and Wagner et al., who highlighted the role of insertional mutagenesis in favoring the expansion and persistence of infected cells in suppressed individuals. Viral integration sites were found to be in intronic regions of MKL2 and BACH2, in the same transcriptional orientation as the host gene, being upstream of the initiation site for

translation for BACH2 and in introns between two coding exons for MKL2, more likely affecting the structure of the protein [24, 54].

Interestingly, Wagner et al. published found that 12.5% of genes targeted by viral integrations were known to be associated with cancer; in particular, integrations were overrepresented in the cancer-associated genes CREBBP, FBX11, and DNMT1, and favored in other 12 genes, namely ANKRD13C, BACH2, C2CD3, CREBBP, HNRNPUL1, IKZF3, KCTD13, MAPK1, OXCT1, STAT5B, ST8SIA4, and TRAPPC10. As far as BACH2 gene is concerned, all these integrations occurred in intron 5 and in the same transcriptional orientation of the BACH2 gene, persisting over time.
The most plausible explanation to this integration pattern is that the cells with the integrations in *MKL2* and *BACH2* were selected post-integration and that the integrations in these genes contributed to the expansion and persistence of the host cells.

We also have characterized the integration profile in peripheral blood mononuclear cells (PBMC) in 54 HIV-infected individuals under cART followed at San Raffaele Hospital in Milan and we detected a total of 13,671 HIV-1/cellular genomic junctions by LAM-PCR. Among the 198 HIV-1 integration sites univocally mapped on the human genome, 3 targeted *BACH2* and 4 targeted *STAT5B*, distributed in 7 patients. Moreover, all the insertions targeting *BACH2* were in the same orientation as gene transcription and 2 of the 3 integrations landed upstream of the first protein coding exon. Regarding integrations targeting *STAT5B*, 3 of the 4 were in the same orientation and all mapped upstream of the first protein coding exon. The analyses then confirmed the tendency of HIV-1 to integrate within gene bodies and in gene-dense regions and we found that out of the 198 integrations retrieved in our study.

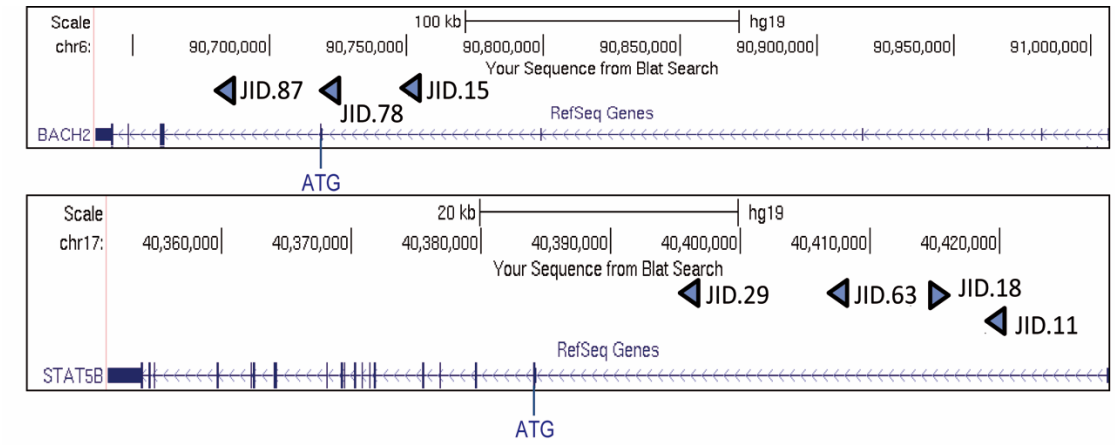


Figure 1.2. HIV-1 integration sites targeting *BACH2* (up) and *STAT5B* (down) found in PBMCs of 54 PLWH under cART. Blue boxes and bars indicate exons, blue arrows indicate the orientation of gene transcription, blue triangles indicate position and orientation of the integration site. Patient ID for each integration site is indicated near the arrow[76].

To sum up, as far as transcriptional orientation is concerned, the viral insertions in *BACH2* were found to be always in the same transcriptional orientation as the host gene, in all the HIV datasets, while *STAT5B* was significantly over-targeted only in ours and in the Ikeda's one. In addition, as almost all viral insertions were within the transcriptional unit of *BACH2* and *STAT5B,* clustered in a tiny genomic window and in the same orientation as transcription, promoter insertion was proposed as the mechanism of activation of these two genes. If it were true, the viral LTR could interfere with the expression of these genes with the generation of chimeric mRNA transcripts containing viral HIV-1 sequences fused by splicing to the first protein-coding exon of the targeted gene downstream of the integration site. Indeed, from the integration analysis performed on mRNAs obtained from PBMCs of a larger cohort of HIV patients (N=87), we found that the transcripts contained the 5' HIV-1 LTR sequences extended until the canonical viral splice donor site and then correctly fused by splicing to the first protein-coding exon of *STAT5B* (exon 2) and *BACH2* (exon 6). Also in this cohort of subjects, the HIV/*STAT5B* and HIV/*BACH2* chimeric transcripts were very abundant, being present in 31%, and 9.2% of the 87 subjects. Notably, 5 patients (5.7%) expressed both and no differences in the frequency of detection of HIV/*STAT5B* (12/48 NT vs 15/39 Exp) and *HIV/BACH2* (4/48 NT vs 4/39 Exp) were observed among the Experienced group with a higher exposure to different ART regimens and the New Therapy group naïve to treatment, suggesting a

minor role of treatment in shaping the reservoir. Finally, we found that *HIV/STAT5B* chimeric transcripts were specifically enriched in regulatory T cells and central memory T cells, as assessed by RT-PCR performed on 9 patients who tested positive for the presence of the chimeric transcripts in the screening. No enrichment of HIV/*STAT5B* was observed in T effector, T naïve, T stem cell memory (Tscm), T effector memory (Tem), total CD8+ T lymphocytes and monocytes. The finding were also confirmed by droplet digital (dd)-PCR: *HIV/STAT5B* and *HIV/BACH2* chimeric mRNAs were found to be enriched in Treg cells in respect to T effector cells (Teff) isolated from 6 HIV-infected patients that resulted positive for the presence of at least one of the chimeric transcripts in PBMCs (ID_25, 77, 76, 32, 38 and 71) at the RT-PCR on samples collected 6 years before, indicating that the cells that harbor this integrations persist over years.

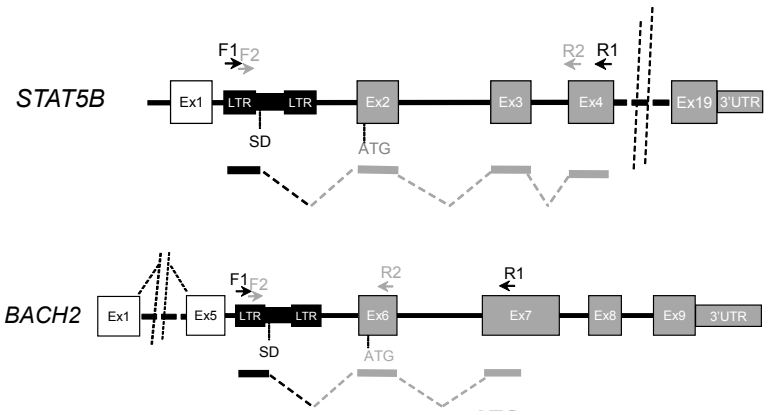


Figure 1.3 Scheme of the RT-PCR strategy used to amplify chimeric HIV/STAT5B or HIV/BACH2 transcripts. Non-coding exons are depicted as white boxes, while coding exons (Ex) are shown in grey. Arrows indicate the positions of the primer pairs. The amplified cDNA sequence derived from the provirus is represented by black bars, whereas the host genome sequence is shown in grey. Dashed lines illustrate the splicing events. LTR: Long Terminal Repeat, SD: 5' major viral splice donor site [76].

To investigate the impact of deregulated STAT5B and BACH2 gene expression in the Treg subset at both functional and molecular levels, bidirectional lentiviral vectors expressing BACH2 or STAT5B were used to transduce in vitro induced Treg cells (iTregs). This approach revealed that the overexpression of the BACH2 and STAT5B transcription factors confers a selective proliferative advantage to Tregs without altering their phenotype or function, demonstrating how HIV-1 facilitates its persistence within the host. Specifically, our findings indicate that BACH2 and STAT5B play a key role in

HIV-1 insertional mutagenesis. Given their biological functions, the HIV-driven overexpression of these genes may contribute to the establishment of a reservoir of infected cells within the Treg compartment.

Treg cells represent a significant viral reservoir due to their long lifespan, higher levels of HIV DNA, and their capacity to produce increased amounts of infectious viral particles upon activation. These characteristics make them an optimal cellular reservoir for HIV persistence. Furthermore, we propose the intriguing possibility that expanded Treg clones may be specific for viral antigens. If so, their proliferation could promote the formation of an HIV-induced immune-tolerant environment, further facilitating viral persistence [76].

Based on these findings, below I report a brief review of the role of the gene BACH2 and STAT5B and of the characteristics and function of the regulatory T and myeloid compartments, specifically in HIV-1 infection.

1.3.3.4.1. Role of the genes BACH2 and STAT5B

BACH2 and *STAT5B* are transcription factors that play a role in cellular growth and survival. In particular, the BTB And CNC Homology 2 *BACH2* gene is located in chromosome 6, composed of 9 exons and only 4 are coding. It is expressed mainly in B-lymphoid cells, specifically from the pro-B cell to the mature B-cell stages but not in the plasma cell stage, and in the fetal brain [77]. *BACH2* can act both as a transcriptional repressor or activator; in B cells acts as a tumour suppressor [78], being involved in diffuse-large-B-cell lymphoma, Burkitt's lymphoma, chronic myeloid leukemia and ovarian cancer [79, 80]. It also regulates immune activation, CD4+ T cell senescence and cytokine homeostasis, maintenance of naïve T cells, limits terminal differentiation preventing T cell exhaustion and potentially promoting the generation of long-lived, highly functional effector-memory T cell population [81]. It is also involved in Treg lineage development and in the differentiation of both thymus-derived Treg cells (tTreg cells) and peripherally-derived T cells (pTreg cells) [81, 82]. Large genome-wide association studies have identified a correlation between specific polymorphisms in the human *BACH2* locus and an increased susceptibility to various autoimmune and allergic diseases, including multiple sclerosis, type 1 diabetes, celiac disease, and Crohn's disease. These findings suggest that BACH2 plays a crucial role in maintaining immunological

tolerance [83]. Additionally, research has shown that reduced tumor growth in Bach2-deficient animals is associated with a lower frequency of FOXP3+ T cells and a higher prevalence of CD4+ and CD8+ effector T cells expressing the cytokine IFNγ within tumors [84].

The Signal Transducer and Activator of Transcription 5B (STAT5B) gene is located on the long arm (q) of chromosome 17 at position 21.2. The protein encoded by this gene belongs to the STAT family of transcription factors. In response to cytokines and growth factors, STAT proteins undergo phosphorylation by receptor-associated kinases, leading to the formation of homo- or heterodimers that translocate into the nucleus, where they function as transcriptional activators. STAT5B specifically mediates signal transduction pathways triggered by various cell ligands and growth hormones.

Mutations or dysregulation of STAT5B have been associated with several diseases, including Growth Hormone Insensitivity with Immunodeficiency and Acute Promyelocytic Leukemia [85].

STAT5 activation plays a critical role in thymic Treg differentiation by facilitating the conversion of FOXP3- Treg progenitors into mature FOXP3+ Tregs through an IL-2/STAT5-dependent mechanism [86]. The significance of IL-2 receptor (IL-2R) signaling in thymic Treg differentiation was demonstrated in Il2rb-deficient mice, which failed to generate thymic Tregs and ultimately succumbed. This phenotype was completely reversed by the introduction of wild-type Tregs [87]. Similarly, crossing Il2rb-/- mice with transgenic mice expressing a constitutively active form of STAT5B restored thymic Treg development [88].

Consistent with these findings, patients with homozygous STAT5B deficiency exhibit reduced FOXP3 expression, along with a decreased number and impaired function of Treg cells [89]. Conversely, transgenic mice expressing a constitutively active form of STAT5B display hyperactive and highly proliferative Treg cells [90].

1.3.3.4.2. Regulatory T and myeloid cells compartment

Previous studies have shown that regulatory T cells (Tregs) represent a specialized subset of CD4+ T cells that develop either in the thymus through MHC class II-dependent T-cell receptor (TCR) interactions or in the periphery through the conversion of naïve CD4+

T cells following TCR stimulation in the presence of transforming growth factor-beta (TGF-β) or dendritic cell-mediated signaling.

Tregs are characterized by high and constitutive expression of the IL-2 receptor α-chain CD25, low levels of the interleukin-7 receptor CD127, and expression of the transcription factor forkhead box P3 (FOXP3). Additional markers involved in Treg-mediated suppression include cytotoxic T lymphocyte-associated antigen-4 (CTLA-4), glycoprotein A repetitions predominant (GARP) receptor, and the glucocorticoid-induced tumor necrosis factor receptor family-related gene (GITR) [91].

Tregs play a crucial role in maintaining immune tolerance through multiple mechanisms: (i) inhibition of T cell proliferation, (ii) production of indoleamine 2,3-dioxygenase (IDO), an enzyme that inhibits T cell activation and proliferation via tryptophan catabolism, promoting peripheral tolerance, (iii) secretion of inhibitory cytokines such as IL-10 and TGF-β, (iv) adenosine production, which contributes to both Treg-mediated immunoregulation and Treg expansion, and (v) use of cytolytic molecules, including granzyme B and perforin, to suppress immune responses, particularly in the context of tumors [92].

Beyond the classical Foxp3-expressing Tregs (Foxp3+ Tregs), several other regulatory T cell subsets have been identified, including type 1 regulatory (Tr1) cells, Th3 cells, CD8+CD28− T cells, human leukocyte antigen (HLA)-G+CD4+ T cells, and HLA-E-specific CD8+ T cells. Among these, Tr1 cells play a key role in peripheral immune tolerance and are distinguished by their ability to secrete high levels of IL-10, which mediates their strong suppressive activity in an IL-10-dependent manner. Unlike Foxp3+ Tregs, Tr1 cells express low levels of IL-4 and IL-17 and do not constitutively express Foxp3 [93].

In the context of HIV infection, the relative frequency of peripheral Tregs increases, particularly in gut mucosa, although their absolute number remains unchanged due to the depletion of CD4+ T cells during both the acute and chronic phases [91]. Given their role in immune regulation, Tregs may suppress chronic immune inflammation in HIV infection while simultaneously dampening HIV-specific immune responses. As a result, their presence is considered beneficial in the early phase of infection but potentially detrimental in the chronic phase [94]. Notably, an imbalance between Th17 and Treg cells

in the intestinal mucosa has been linked to disease progression, with the Th17/Treg ratio serving as a predictor of immune activation in individuals with primary HIV infection [95, 96].

Tregs have also been proposed as a cellular reservoir for HIV persistence, as the frequency of HIV DNA-harboring cells is higher in the resting Treg compartment compared to non-Treg subsets. Furthermore, the estimated half-life of latent HIV-infected Tregs is approximately 20 months, which is comparable to other non-Treg reservoirs and sufficiently long to sustain viral persistence despite cART [97].

Conversely, subsets of myeloid cells with regulatory functions, collectively known as myeloid regulatory cells (MRCs), have been identified and characterized in immune-mediated diseases across all major myeloid lineages, including polymorphonuclear neutrophils (PMNs), macrophages, and dendritic cells (DCs). Among these, a specific subset termed myeloid-derived suppressor cells (MDSCs) has been found to promote a tolerogenic microenvironment that supports the expansion of Tregs [98].

Tissue-resident macrophages are categorized based on their activation state: pro-inflammatory or classically activated (M1) macrophages and anti-inflammatory or alternatively activated (M2) macrophages. While M1 macrophages are involved in immune defense and inflammation, M2 macrophages are associated with processes such as fibrosis, allergic responses, and tumor progression.

Monocytes, a highly heterogeneous population, are classified into three subsets: ‘classical’ inflammatory monocytes (CD14highCD16−), which make up 80% of circulating monocytes and exhibit phagocytic activity while secreting pro-inflammatory cytokines; ‘intermediate’ monocytes (CD14+CD16+), which retain regulatory function and secrete IL-10, and ‘non-classical’ monocytes (CD14lowCD16+), which are specialized in patrolling the endothelium for signs of damage and infection. Intermediate monocytes are further distinguished by the expression of Ly6ChighCD43high, whereas non-classical monocytes are characterized by Ly6ClowCX3CR1highCCR2lowCD43high expression [99]. Classical CD14highCD16− monocytes contribute to a pro-inflammatory environment in autoimmune disorders by promoting the conversion of resident M2 macrophages into M1 macrophages. They have been found in elevated numbers in the synovial fluid of patients with rheumatoid arthritis

(RA), the inflamed mucosa of individuals with inflammatory bowel disease (IBD), and the central nervous system (CNS) of patients with relapsing-remitting multiple sclerosis (MS) [100-102]. Conversely, an expansion of intermediate CD14+CD16+ monocytes correlates with disease severity in IBD, RA, and psoriasis [103]. Additionally, a reduction in classical CD14+CD16− monocytes, along with an increase in non-classical CD14lowCD16+ monocytes, has been described in patients with RA responding to treatment [104].

Dendritic cells (DCs) act as messengers between the innate and adaptive immune systems by capturing and internalizing pathogens, processing their antigens, and presenting them via major histocompatibility complex (MHC) class I and class II molecules to CD8+ and CD4+ T cells, respectively [105]. These antigen-presenting cells (APCs) originate from bone marrow progenitors (BMP) and circulate in the bloodstream as immature precursors before migrating into peripheral tissues. For instance, they populate the skin as epidermal CD207+ Langerhans cells (LCs) and the lamina propria of the small intestine [106]. Positioned at the interface with the environment, DCs function as sentinels of the immune system. Upon receiving appropriate stimuli, they undergo maturation, migrate to secondary lymphoid organs, and initiate adaptive immune responses by activating CD8+ and CD4+ T cells [107].

However, immature DCs that migrate to lymph nodes at low frequencies without undergoing activation present antigens to T cells in the absence of co-stimulatory signals, thereby inducing clonal T-cell anergy or promoting the differentiation of Tregs [108, 109].

In peripheral blood, at least two major subsets of pro-inflammatory DCs function as APCs: CD11c+ conventional DCs (cDCs), which express either CD1c (blood dendritic cell antigen-1, BDCA-1) or CD141 (BDCA3), and CD11c−CD123+ plasmacytoid DCs (pDCs), which express BDCA-2, BDCA-4, and CD123 (the interleukin-3 receptor, IL-3R) and are potent producers of type I interferons (IFN) in response to foreign antigens [110].

Alongside these pro-inflammatory DC subsets, a distinct subset of human tolerogenic DCs, known as DC-10, has been characterized by its ability to spontaneously secrete large amounts of IL-10 [111]. IL-10, a key immunomodulatory cytokine, is produced by

various leukocytes, including T cells, monocytes, macrophages, DCs, B cells, natural killer (NK) cells, mast cells, neutrophils, and eosinophils [112]. IL-10 promotes immune tolerance through multiple mechanisms: (i) downregulating the expression of MHC class II and co-stimulatory molecules CD80 and CD86 on DCs; (ii) inhibiting the release of pro-inflammatory cytokines such as IL-1β, IL-6, TNFα, and IL-12 by DCs; (iii) inducing anergic T cells with suppressive activity in vitro [113, 114]; (iv) upregulating IL-10 production while increasing the expression of HLA-G, ILT2, ILT4, and HO-1 on DC precursors, thereby enhancing their regulatory function and facilitating Treg induction [115-118]; and (v) modulating DC differentiation by promoting the expression of markers such as CD83 and BDCA-3 [119, 120].

DC-10 can be generated in vitro from peripheral blood monocytes and are characterized by CD14 and CD16 expression, while lacking CD1a. They exhibit a mature myeloid phenotype, expressing CD83, CD86, and HLA-DR, even in the absence of activation stimuli. In vivo, functional DC-10 can be identified by the co-expression of CD141 and CD163 alongside CD14 and CD16 [121]. Furthermore, DC-10 express high levels of HLA-G and other tolerogenic molecules such as ILT2, ILT3, and ILT4, whose elevated expression, together with IL-10 production, is essential for their tolerogenic function and their ability to induce Tr1 cells via the IL-10-dependent HLA-G/ILT4 pathway [111]. HLA-G is an immunomodulatory molecule that regulates both innate and adaptive immune responses and promotes immune tolerance [122].

DC-10 cells are found in peripheral blood, in secondary lymphoid organs of healthy individuals and in the human decidua during the first trimester of pregnancy [123]. An elevated frequency of DC-10 cells has been observed in patients with acute myeloid leukemia, particularly in those with HLA-G-expressing blasts compared to those with HLA-G-negative blasts [124]. Based on these observations, it is suggested that HLA-G-expressing DC-10 cells may play a role in maintaining HLA-G expression on leukemic blasts, thereby influencing the immune response and aiding in tumor immune evasion. Supporting this idea, DC-10 cells with high levels of HLA-G have been found in greater numbers in the blood of gastric cancer patients and are linked to more advanced disease stages [125]. Additionally, studies have demonstrated a reduced frequency and number of circulating DC-10 in pediatric patients with type 1 diabetes (T1D) at disease onset, as well as in individuals at risk of developing the condition [126].

Hence, DC-10 can be used as a therapeutic tool to induce or re-establish immunological tolerance in allogeneic transplantation or autoimmune diseases.

The role and contribution of dendritic cells (DCs) in HIV-1 infection remain uncertain. On one hand, certain subpopulations of DCs located in the genital mucosa are a preferred target of HIV, with a role in sexual transmission [127]. Additionally, DCs can transfer HIV-1 particles to CD4 T cells through the process of trans-infection [128].

DCs are significantly reduced in untreated PLWH, with the depletion of circulating cDCs correlating with rapid disease progression in HIV-1 infection [129-131]. Notably, DCs contain mechanisms that detect HIV-1 replication products, which may play a key role in generating both cellular and humoral immune responses in elite controllers [132]. HIV-1 appears to alter plasmacytoid DCs (pDCs), making them more tolerogenic and promoting the polarization of CD4+ T cells into immunosuppressive regulatory T cells [133]. Conversely, cDCs from HIV-1 elite controllers have been shown to retain effective antigen-presenting functions, stimulating HIV-specific CD8+ T cells in these patients. [134]. On the other hand, the abnormal activation of DCs may contribute to ongoing inflammation and immune activation. Interestingly, infected DCs interact with T cells from HIV-1-infected individuals to promote the production of IL-10 and immune suppression [135]. Additionally, an increase in monocytes expressing HLA-G was observed in PLWH receiving HAART, a change not seen in untreated patients. These findings were further confirmed when antiretroviral treatment was interrupted, as the number of peripheral monocytes expressing HLA-G progressively decreased. This suggests that HAART can induce the expression of the tolerogenic molecule HLA-G on peripheral monocytes in PLWH [136].

Moreover, DCs exposed to HIV exhibited a more tolerogenic phenotype, showing increased expression of PDL1, Gal-9, HVEM, and B7H3. This change was mediated through interactions with T cells and may contribute to the suppression of immune responses observed in PLWH [137].

2. AIM OF THE STUDY

Previous research performed in the laboratory of Safety of gene therapy and insertional mutagenesis research unit of the San Raffaele Telethon Institute for Gene Therapy (TIGET), where I conducted this thesis project, demonstrated a significant enrichment of HIV-1 integrations targeting *STAT5B* and *BACH2* in PBMC obtained from HIV-infected individuals under ART. Plus, the chimeric mRNA transcripts resulting from the fusion of the HIV-1 sequences to the first protein-coding exon of *STAT5B* or *BACH2* were enriched in Tregs and in central memory T cells. Indeed, we showed that HIV deregulates targeted gene *BACH2* and *STAT5B* by insertional mutagenesis, providing a selective proliferative advantage in Tregs. On the other hand, initiating ART early during acute infection supports immunological recovery, reduces the size of the HIV reservoir, and enhances the likelihood of post-treatment viral control compared to individuals who begin ART during chronic infection.

Considering the emerging role of regulatory T cells in maintaining the HIV reservoir, this thesis seeks to characterize the composition of regulatory lymphocytic and myeloid compartments. We will quantify and analyze the HIV reservoir, distinguishing between intact and defective proviruses, and examine whether the timing of ART initiation, either in acute or chronic infection, affects the intactness of the reservoir. Additionally, we seek to gain a deeper understanding of the mechanisms that drive HIV persistence during both acute and chronic stages of infection, by analyzing the HIV-1 integration profile and identifying potential molecular targets involved in this process.

Another approach to tame the reservoir is through immunological control. Here, we explore whether KIR-HLA combinations may be associated to a better immune recovery, underlying a potential impact on the ability to control HIV replication and the formation of the HIV reservoir. KIR-HLA combinations could represent potential markers of post-treatment control.

In brief, the thesis strives to provide a deeper understanding of the immune mechanisms that support HIV persistence and control, as well as identifying potential targets for therapeutic strategies aimed at eradicating or controlling HIV infection more effectively. To achieve these objectives, we designed and conducted the PERSHIST study and I contributed as a sub-investigator to the IMMUNERaRe study.

3. MATERIALS AND METHODS

3.1. PERSHIST study

PERSHIST study is a non-pharmacological interventional, transversal, genetic, and monocentric study involving people with HIV, followed at the Infectious Diseases Clinic of OSR. Primary aim of the study is to generate a database of genes highly targeted by HIV-1 integrations and chimeric virus/host mRNA sequences in different subpopulations of hematopoietic cells isolated from peripheral blood of people with HIV.

We enrolled adult people living with HIV (PLWH) on virological suppression under ART and with a good immunological profile (CD4 >500 cells/ μL), followed at the Department of Infectious Diseases of IRCCS San Raffaele Institute (Milan, Italy).

Participants were stratified in three groups:

1. people with chronic HIV infection receiving ART >15 years and with suppressed HIV-RNA (less than 50 copies/mL for at least 3 years), (Group 1);
2. people with chronic HIV infection receiving ART >5 years and with suppessed HIV-RNA (less than 50 copies/mL for at least 2 years), (Group 2);
3. people with acute HIV infection receiving ART >2 years and with suppressed HIV-RNA (less than 50 copies/mL for at least 1 year), (Group 3).

The inclusion criteria were as follows: (1) age 18 or over; (2) able to sign an informed consent; (3) clinical characteristics fitting with the above- mentioned categorizations. The exclusion criteria were as follows: (1) not able to sign an informed consent; (2) clinical characteristics not fitting with the above- mentioned categorizations; (3) acute or chronic HCV and/or HBV co-infection; (4) leukapheresis contraindicated (i.e. history of epilepsy, intolerance to citrate or psoralene, absence of central line access or large peripheral lines, severe renal or cardiac diseases, hemodynamic instability or septicemia, diarrhea >1 L/die resulting in hemodynamic instability, electrolyte imbalance not treatable with a short-term infusion replacement; anemia with haemoglobin < 8 g/dL and thrombocytopenia with platelet count <20.000/mmc or lymphopenia with blood cell count <1000/mmc, use of angiotensin-converting enzyme inhibitor and sartans in previous 48 hours). At enrollment a blood sample and a leukapheresis were performed for the cytofluorimetric analysis and the integration analyses, respectively. As control group, we included PLWH without HIV.

After the informed consent is signed, blood sample will be collected through venepuncture or though apheresis, following the standard procedure outlined in IOS SIMT 015. The apheresis will be carried out at the OSR Hematology outpatient clinic (Dr. Milena Coppola). The storage of the blood samples will be managed by the TIGET research laboratory (Dr. Daniela Cesana).
Anonymized data from the CSL HIV Cohort, sourced from the Infectious Diseases Department database of IRCCS San Raffaele Scientific Institute, were analyzed. The study received approval from the ethics committee of IRCCS San Raffaele Scientific Institute (protocol Version 1.0, November 9, 2016), and all participants gave written informed consent.

3.1. IMMUNERaRe study

ImmuneRaRe is a proof-of-concept study that explores a range of biomarkers, including immune-genetic and viro-immunologic markers, which could help identify PTCs. It consists of two steps: the first step, which is the focus of this work, is an observational, mono-centric research study involving individuals with primary HIV infection who are followed at the Infectious Diseases Clinic of Ospedale San Raffaele, Milan, Italy. The second step is a prospective, interventional, mono-centric, phase 4, controlled clinical study, which is currently ongoing.
According to immunological recovery after ART start, participants were stratified in three groups:

- Rapid Responders (RR), when CD4/CD8 ratio and absolute count of CD4+ and CD8+ T cells and were within normal laboratory range within 8/12 weeks from cART initiation;
- Conventional Responders (CR), when CD4/CD8 ratio and absolute count of CD4+ and CD8+ T cells were within normal laboratory range after 12 weeks and within 48 weeks from cART initiation;
- Immunological non-Responders, when all three parameters were not normalized within 48 weeks.

Normal laboratory ranges for CD4 and CD8 count are 493-1666 cells/microL and 224-1112 cells/microL. CD4/CD8 ratio was considered to be normalized when above 1.

The inclusion criteria were as follows: (1) individuals aged 18-70 years, regardless of gender; (2) confirmed HIV-1 seropositivity; (3) initiation of ART during primary HIV infection, defined by Fiebig stage; (4) undetectable plasma HIV-RNA (< 50 copies/ml) for at least 24 months; (5) CD4+ T cell absolute count > 350 cells/mm³ at the most recent routine follow-up visit; (6) absence of new AIDS-defining conditions or progression of the HIV-related disease; (7) ability to adhere to an effective ART regimen for the study's duration; (8) willingness and capacity to provide written informed consent for study participation.

The exclusion criteria were as follows: (1) confirmed HIV-2 seropositivity; (2) pregnant women; (3) a history of systemic cancers, such as lymphoma or Kaposi's sarcoma, other virus-associated malignancies, and/or a history of AIDS-defining illnesses as per CDC criteria; (4) active or chronic HBV infection, indicated by detectable HBV surface antigen or HBV DNA, active or chronic HCV infection with detectable viral RNA, and syphilis.

The AHI database of the Infectious Diseases Clinics was accessed to identify all the patients that meet the proposed selection criteria and can be enrolled in this observational study. Starting from the signature of the informed consent by the patient, the subjects was considered enrolled in the clinical trial and a blood donation of 100 ml was withdrawn. Clinical and routine tests results (HIV-1 RNA load, tropism test, genotype ART resistance test), immunological (CD4+, CD4%, CD8+, CD8%, CD4/CD8) and genetic data (CCR5 genotype) are recorded at enrollment. The blood donation has been transferred in the laboratory of the VET Unit, processed by fully trained personnel that will collect plasma, serum and PBMCs either as dry pellet for genetic analysis or living cells for all FACS analysis.

A secondary endpoint of the study is the validation of the immune-genetics platform for genotyping KIRs/SNPs that regulate HLA-C expression, as well as HLA A-B-C typing, in a clinical setting, performed in collaboration with the laboratory of Molecular Diagnostic, IRCCS Gianna Gaslini.

In particular, one aliquot of dried pelleted PBMC for each patient was sent to IRCCS G. Gaslini for nucleic acid extraction and testing for KIR genotyping, HLA typing, and SNPs rs67384697 G/- and SNP rs2395471 A/G affecting HLA-C expression. Moreover, quantification of intact and defective DNA viral genome in CD4 T cells was also performed in collaboration with Laboratory of Safety of gene therapy and insertional

mutagenesis Unit. In particular, 15 to 30 millions of cryopreserved PBMCs were used for each patient to perform IPDA.

3.3. Lab Methods

3.3.1. Cell purification and cytofluorimetric analysis

Naïve CD4+ T cells were isolated from 120-200 mL of EDTA-treated peripheral blood from the enrolled subjects after lymphocyte apheresis, and from 50 mL of buffy coat of a healthy donor using Ficoll-Hypaque gradient separation. The T cells were then purified from the PBMCs through magnetic cell sorting using the CD4+ Isolation Kit (Miltenyi). From the cell suspension removed by the leukapheresis, regulatory T cells (Treg), effector T cells (Teff), naïve T cells, T memory stem cells (Tscm), central memory T cells (Tcm), T effettor memory T cells (Tem), were sorted by FACS, with a purity superior to 90% for every subtype.

In particular, CD4 T-effector ($CD4^+$ $CD25^-$), Treg ($CD4^+$ $CD25^+$ $CD127^-$) and $CD8^+$ T cells were isolated by FACS sorting following staining of PBMC with fluorescent anti-CD3 (1:100 dilution, cod. 345765, BD Biosciences), anti-CD4 (PRJNA392654), anti-CD25 (1:100 dilution, cod. 340907, BD Biosciences), and anti-CD127 (1:100 dilution, cod. 25 12 78 42, Ebioscience) and anti-CD8 (1:100 dilution, cod. 558116, BD Biosciences). T stem cell memory, T naive, T central memory, and T effector memory cells were isolated by FACS from an enriched fraction of $CD4^+$ cells, isolated with lineage-specific kit (Miltenyi Biotech). $CD4^+$ cells were recognized with anti-CD8 (1:100 dilution, cod. 555368, BD Biosciences), anti-CD45RA (cod. 560362, 1:100 dilution, BD Biosciences), anti-CD4 (1:50 dilution, cod.317418, Biolegend), anti-CD95 (1:100 dilution, cod. 305608, Biolegend), and anti-CD62L (1:100 dilution, cod. 1A-449-T100, Exbio) fluorescent mAbs. The different subsets of T cell were determined by the following markers: T naïve, $CD4^+CD45RA^+CD62L^+CD95^-$; Tcm, $CD4^+CD45RA^-CD62L^+$; Tscm, $CD4^+CD45RA^+CD62L^+CD95^+$; and Tem, $CD4^+CD45RA^-CD62L^-$. BD FACSAria cell sorter was used for cell sorting.

In order to increase the yield, naive T cells, Treg, and Teff and the CD8+ T cells and monocytes were separated also through the use of magnetic beads, utilizing lineage-

specific kits (Miltenyi Biotec). Flow cytometric analysis was used to evaluate the purity of each fraction.

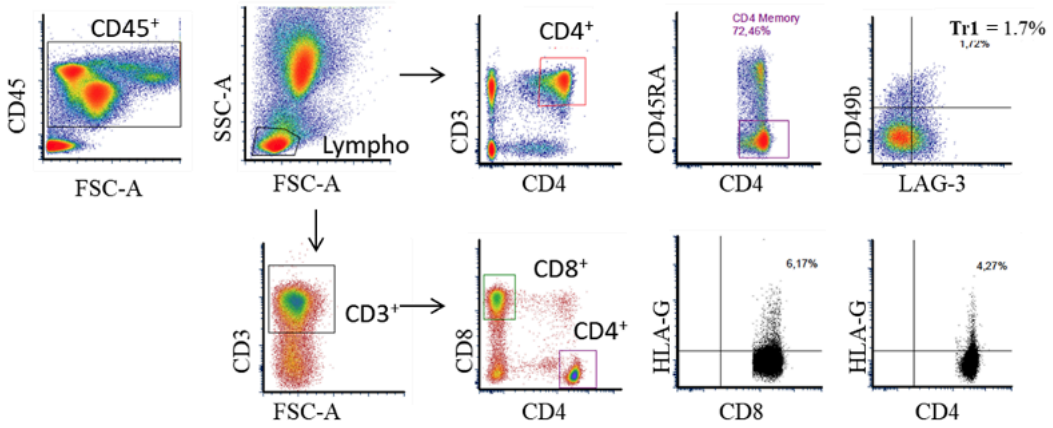


Figure 3.1. Scheme of gating strategy for the selection of CD4+ e CD8+ T cells.

The frequencies of DC-10 and other myeloid populations, along with the expression levels of HLA-G, CD83, ILT4, and HLA-DR, were assessed in EDTA-treated peripheral blood. PBMC staining was carried out using anti-CD1c, CD16, CD14, HLA-DR, CD163 (Becton Dickinson, CA, USA), and CD11c, CD141 (Miltenyi Biotech, Germany). Denditric cells (DC) co-expressing CD11c, CD16, CD14, CD163 and CD141 were defined as DC-10. DC identified as CD14- were distinguished into cDC1 if co-expressing CD11c and CD141 (BDCA-3) and as cDC2 when co-expressing CD11c e CD1c (BDCA-1). HLA-DR expression was separately evaluated. Analyses were performed by FACSCanto II flow cytometer (Becton Dickinson, Mountain View, CA).

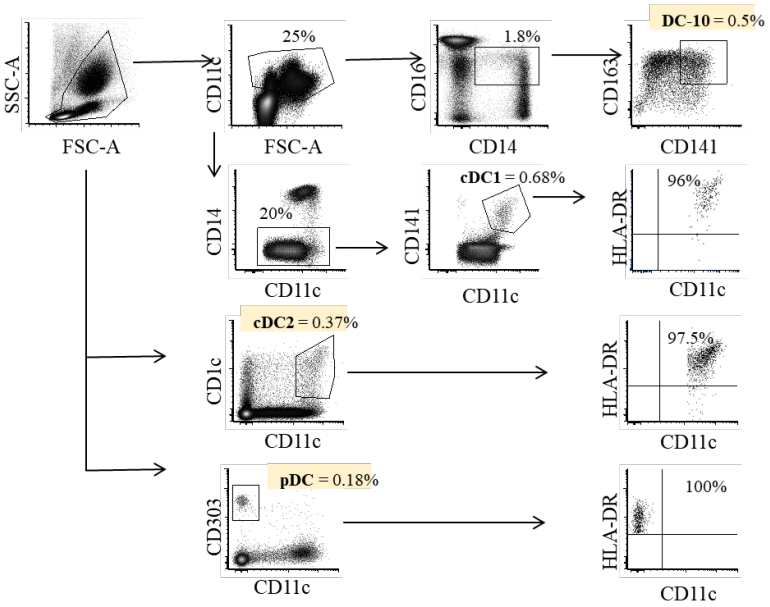


Figure 3.2. Schematic of gating strategy for the selection of the cellular component of the myeloid cellular subtypes analyzed.

In this study, cytofluorimetric analysis was employed to evaluate the relative composition of specific lymphocytic and myeloid subpopulations in Group 1-3, and these were compared to healthy donors.

3.3.2. Intact proviral DNA assay

According to the method described in Bruner et al. [44], The intact proviral DNA assay (IPDA) utilizes the droplet digital PCR (ddPCR) method to differentiate between deleted and intact proviruses using two amplicon probes derived from genomic DNA (gDNA). Genomic DNA was extracted using the QIAamp DNA Mini Kit (Qiagen), with precautions taken to prevent excessive DNA fragmentation. DNA concentrations were determined using the Qubit 3.0 and Qubit dsDNA BR Assay Kit (ThermoFisher Scientific). The IPDA was conducted on DNA from 5×10^6 CD4+ T cells, with 500 ng of genomic DNA analyzed in each reaction well, in a volume of 20 µL.

Quantification of intact, 5′ deleted, and 3′ deleted proviruses is carried out using primer/probe combinations optimized for subtype B HIV-1 (Accelevir Diagnostics).

Custom-made locus specific ddPCR assays were used to target Ψ region positioned at HXB2 coordinates 692–797 and *env* region at the RRE, with the amplicon positioned at HXB2 coordinates 7736– 7851. The reactions use forward and reverse primers, together with a 5′ 6-FAM-labelled hydrolysis probe and a 5′ HEX-labelled hydrolysis probe whose fluorescence is detected by droplet reader.

7 ng of DNA for each sample was used in each reaction well to test the abundance levels of the reference gene *RPP30*; the reactions use forward and reverse primers, as well as a 5′ 6-FAM-labelled hydrolysis probe and a 5′ HEX-labelled hydrolysis probe whose fluorescence is detected by droplet reader. A maximum of 20,000 monodispersed droplets per sample were generated using the QuantaLife droplet generator and amplified to endpoint in a standard thermal cycler (Bio-Rad QX200 AutoDG Digital Droplet PCR system). The amplification was carried out with the appropriate manufacturer-supplied consumables and ddPCR Supermix for probes, following the conditions outlined below: 1 cycle for 10 mins at 95°C for enzyme activation, 45 cycles for 30 seconds at 94°C for

denaturation and for 1 minute at 59°C for annealing or extension, 1 cycle for 10 mins at 98°C for enzyme deactivation and hold at 4-12°C.

Reactions were performed in triplicate wells to ensure consistent quantification.

The gating for positive droplets was determined using HIV-seronegative CD4 T-cell and PBMC DNA-negative control wells, which were included on each digital PCR plate. Given the occasional detection of low-amplitude false-positive droplets in negative control wells at a rate of 0–5 copies per million cells, the mean of the values obtained from the negative controls was calculated. Any values falling below this mean were considered undetectable.

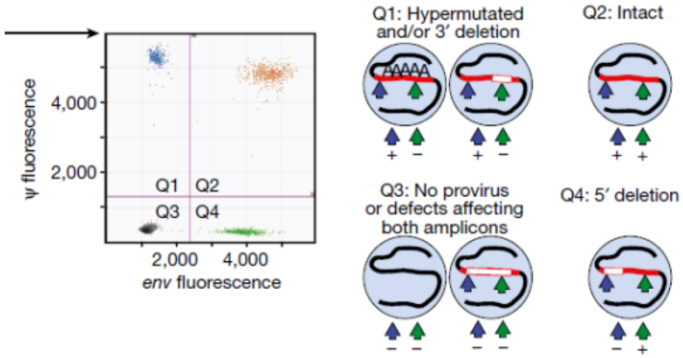


Figure 3.3. Illustration of ddPCR plot showing intact (Q2) and defective proviruses (Q1 and Q4) by IPDA.

3.3.3. Sonicated Linker Mediated (SLiM)-PCR for the identification of integration sites and library preparation

The Sonicated Linker Mediated (SLiM)-PCR is based on the method published by Firouzi at al. [137], it encompasses the casual fragmentation of the genomic DNA extracted from cells harboring the viral integration by ultrasonication.

10 DNA samples extracted from CD4+ T cells purified from the enrolled patients (L002 to L011) were processed by SLiM-PCR.

Following isolation of genomic DNA from PBMC by QIAamp DNA Midi and Mini kit, the concentration was measured with NanoDrop 2000 spectrophotometer (Thermo Scientific). Genomic DNA was sheared using a Covaris E220 Ultrasonicator in order to reach a target peak of 1000 bp, under specific conditions (Peak Incident Power: 175; Duty Factor: 2%; Cycles per Burst: 200; Treatment Time: 45 seconds; Temperature 7°C; Water level: 6; E220 Intensifier). Sonicated DNA was subjected to end repair, adenylation and ligation to barcoded linker cassettes using the NEBNext® Ultra™ DNA Library Prep Kit

for Illumina® following manufacturer instructions. In particular, a synthetic linker cassette is attached to each fragment, being made of a 8 bp ds-DNA cassette of known sequence, an Illumina barcode and, differently from Farouzi et al., we also have inserted during the ligation step a random sequence of 12 nucleotides, defined as unique molecular modifier (UMI), allowing for the identification of each fragment (Schematic representation in figure 3.3.).

Moreover, being HIV a highly mutagenic virus with mutations also in the LTR sequence, we have designed patient-specific primers, using as a template the sequence of the LTR obtained by the chimeric transcripts identified (see Chapter 4.3) to increase the efficiency of the technique. Different barcodes were used to distinguish technical replicates of the same sample. In this way, during the amplification reaction, we amplify specifically the genomic fragments that harbor the junction virus/cell genome and we are able to quantify the number of fragments with the same IS, which are proportional to the number of infected cells that carry that specific integration.

The ligation products underwent 35 cycles of exponential touchdown PCR using specific primers for the LTR and LC. The amplification products were then re-amplified for an additional 20 PCR cycles using an inner primer specific to the inner LC and HIV genome (barcoded fusion primer). Each Fusion-primer PCR product was quantified by qPCR (Kapa Biosystems), following the manufacturer's instructions. Samples were diluted 10,000 times in 10 mM Tris-HCl and quantified in technical triplicates on a 384-well plate. The qPCR plate was analyzed using a Thermo Fisher Viia7 Real-Time PCR System. Based on the qPCR quantification, different volumes of the SLiM-PCR products were pooled in equimolar ratio in three sequencing libraries. By bioinformatics tools, the amplification products were sequenced by NovaSeq Illumina Platform and mapped to the reference human genome, implemented from the one described by Spinozzi et al. [138].

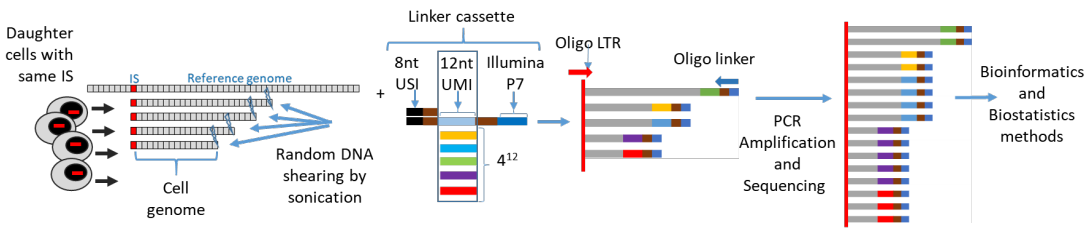


Figure 3.4. Schematic of the SLiM-PCR.

3.3.4. Chimeric transcripts retrieval

Total RNA was extracted from CD4+ T cells isolated from all subjects using RNeasy purification kits (Qiagen). A total of 300 ng of RNA was reverse-transcribed with the High Capacity cDNA Reverse Transcription Kit (Invitrogen). For qualitative PCR, 120 ng of cDNA was used as the template.

Amplification was carried out in a total volume of 50 µL using Taq polymerase (Qiagen). A second nested PCR amplification was performed using 3 µL of the first PCR reaction. Both the first and second PCR cycles were conducted in a standard thermal cycler (Bio-Rad) under the following conditions: an initial 5-minute denaturation at 95°C, followed by 40 cycles of 30 seconds at 95°C, 60 seconds at 54 or 58°C (depending on the oligos used), 30 seconds at 72°C, and a final extension at 72°C for 10 minutes, with a hold at 4°C.

The oligoes used for the nested PCR are the following:
STAT5B I: 5' CATTGTTGGCTTCTCGGACC 3'
STAT5B II: 5' GGGCAGCGGTCATACGTG 3'

BACH2 I: 5' CAGCTTGGCAGTGTAGGC 3'
BACH2 II: 5' CCCTGGCTGTGACCTCCTC 3'

HIV-I: 5' GAGCTGTCTGGCTAACTAGG 3'
HIV-II: 5’ AGCTTGCCTTGAGTGCTTCA 3’

PCR fragments were purified with agarose gel. Subsequently, Illumina barcodes were attached to the amplified products by TruSeq Nano DNA LT Sample Prep Kit (Illumina). Samples were pooled in different libraries. Sequencing was performed using an Illumina MySeq platform. By bioinformatics tools, the reads were aligned against a reference sequence.

3.4. Statistical Analysis

Descriptive analyses were conducted according to the study arm, with endpoints summarized using medians with interquartile ranges, ranges, or 95% confidence intervals (CI) for quantitative variables, and proportions with their corresponding 95% CI for qualitative or categorical variables. Confidence intervals were calculated using the exact method. Due to the small sample size of the study groups, the analyses were primarily descriptive, as the study lacked the statistical power for formal hypothesis testing to assess differences between groups.

The analyses focused on identifying clinically relevant differences in key baseline characteristics among study groups. If significant imbalances were observed, statistical tests were applied accordingly: categorical variables were evaluated using the chi-square test or Fisher's exact test, while continuous variables were assessed using the non-parametric Wilcoxon rank-sum test or Kruskal-Wallis test. Additionally, Spearman's rank correlation coefficients were used to explore relationships between different study outcomes.

Most of the analyses were conducted using GraphPad Prism and R software. For any additional statistical considerations arising during the experiments, support was sought from a statistician at the Department of Infectious Diseases at IRCCS San Raffaele Scientific Institute.

1. RESULTS

4.1. PERSHIST study

4.1.1. Characteristics of the cohort

In this study, adult people living with HIV (PLWH) on virological suppression under ART and with a good immunological profile (CD4 >500 cells/ µL) were enrolled. All these patients are followed at the Department of Infectious Diseases of IRCCS San Raffaele Institute (Milan, Italy).

Participants were stratified in three groups:

1) people with chronic HIV infection receiving ART >15 years and with HIV RNA <50

copies/mL >3 years (Group 1);
2) people with chronic HIV infection receiving ART >5 years and with HIV RNA <50 copies/mL >2 years (Group 2);
3) people treated during acute HIV infection, receiving ART since at least 2 years and with HIV RNA <50 copies/mL >1 year (Group 3).

Among 28 PLWH enrolled, 8 (28.6%) belong to Group 1, 11 (39.3%) to Group 2 and 9 (32.1%) to Group 3 (Patients characteristics reported in Table 4.1). All participants were male and median (IQR) age at enrollment was 51.0 (42.0-55.0) years. Median year of ART start after diagnosis was 5.4 (0.7-39.0) with a median CD4 nadir of 256 (184-360) cell/μL and HIV-RNA at HIV diagnosis 93150 (48814.7- 598671.5) copies/mL (Table 4.1). All participants showed optimal immune-virological parameters at enrollment (Table 4.2).

Group	ID	Age	Gender	CDC classif.	Date of diagnosis	CD4 nadir (cells/µL)	Viremia at diagnosis (copies/mL)	Months to ART start	Years of ART	Years of HIV RNA <50copies/mL	Total CD4 at enrollment (cells/µL)	CD4 (%) at enrollment	CD4/CD8 ratio at enrollment	Subtype
1	L002	52	M	B1	10/01/95	280	340000	57.8	21.8	15.8	1392	46.4	1.7	B
	L004	53	M	B1	02/09/04	250	NA	34.2	16.8	13.7	694	40.8	0.9	NA
	L014	44	M	A3	02/03/09	72	535962	5.8	15.2	14.8	714	34	1.03	B
	L021	69	M	B3	06/09/00	16	430000	0.4	22.6	21.6	958	39.9	2.91	B
	L024	57	M	NA	19/03/96	NA	NA	148.7	26.8	17	664	30.2	0.77	NA
	L025	64	M	C3	01/01/97	NA	NA	24.3	26	12.6	719	32.7	0.76	B
	L027	53	M	NA	22/06/05	NA	NA	70	17.1	NA	641	35.6	1.35	B
	L028	60	M	B2	27/03/02	256	81000	3.6	20.9	20.8	909	41.3	1.59	B
2	L005	43	M	A1	5/18/2009	123	478882	54.3	8.5	8.2	1796	49.9	2.5	B
	L006	50	M	B1	04/02/12	278	13000	184.6	5.7	5.5	570	25.9	0.8	B
	L008	51	M	B1	10/11/10	184	63664	5.8	7.4	6.9	1369	37.0	1.0	B
	L009	50	M	C1	3/17/2010	58	2100	2.9	8.0	7.5	1146	39.5	1.1	B
	L010	43	M	A1	10/04/10	73	2000000	83.9	7.6	7.4	1572	58.5	2.9	NA
	L011	38	M	A1	9/26/2011	428	105300	54.1	6.7	6.1	464	27.3	0.7	B
	L013	39	M	A1	07/09/12	260	46780	5.6	6.2	5.9	961	31.0	1.2	B
	L015	63	M	A2	30/12/11	246	207900	0.6	11.7	11.6	762	40.1	0.85	B
	L016	37	M	B2	16/01/14	237	75140	12.4	9.8	9.6	793	31.7	0.72	B
	L019	33	M	A2	21/01/15	282	75058	2	8	7.6	832	37.8	1.52	B
	L023	55	M	A2	06/11/12	270	12960	5.2	10.6	10.6	686	26.4	0.6	B
3	L001	47	M	B1	11/20/2009	396	8667	0.6	7.5	7.2	796	37.9	1.9	NA
	L003	53	M	B1	9/25/2015	127	55716	0.7	2.1	1.9	700	31.0	1.0	C
	L007	40	M	A1	7/27/2009	545	2000000	0.1	8.6	8.3	961	31.0	1.2	NA
	L012	37	M	A1	01/09/14	530	14720	0.1	4.2	3.9	377	15.7	0.3	B
	L017	51	M	A2	05/08/11	360	1003000	0.3	12.5	12	698	34.9	1.18	B
	L018	44	M	A2	06/10/10	252	786800	3.9	12.6	11.8	632	39.5	1.2	B
	L020	55	M	A2	10/12/09	224	49493	30.9	13.3	12.8	602	25.1	0.5	NA
	L022	66	M	A2	08/09/09	459	1316000	4.1	13.5	13.2	774	45.5	1.94	B
	L026	33	M	A2	01/07/13	454	1095000	0.3	10.1	9	1421	41.8	1.34	B
Overall	Median (IQR)	51.0 (42.0-55.0)	-	-	2010 (2007-2012)	256 (184-360)	93150 (48814.7-598671.5)	5.4 (0.7-39.0)	10.35 (7.57-14.0)	9.6 (7.3-13.0)	768.0 (681.0-961.0)	36.3 (31.0-40.0)	1.14 (0.79-1.53)	-

Table 4.1. Participants' characteristics stratified for each group. ID: patient identifier. ART: antiretroviral therapy. NA: not available.

		Group 1 N=8	**Group 2 N=11**	**Group 3 N=9**	p. value
Age		55 [53-61]	43 [38,5-50,5]	47 [40-53]	0.416
Months from HIV diagnosis to ART start		29,25 [5,25-60,85]	5,8 [4,05-54,2]	0,6 [0,3-3,9]	0.165
HIV-RNA at diagnosis	Copies/mL	385.000 [309.000-456.490,5]	75.058 [29.890-156.600]	786.800 [49.493-1.095.000]	0.332
CD4 count nadir	Cells/mm^3	250 [72-256]	246 [153,5-274]	396 [252-459]	0.013
CD4 count at enrollment	Cells/mm^3	716,5 [686,5-921,25]	832 [724-1257,5]	700 [632-796]	0.125
CD4 percentage at enrollment	%	37,75 [33,67-40,92]	37 [29,15-39,8]	34,9[31-39,5]	0.510
CD4/CD8 at enrollment		1,19 [0,8675-1,6175]	1 [0,76-1,36]	1,2 [1-1,34]	0.832

Table 4.2. Comparison among groups was performed using Kruskal-Wallis test for continuous variables. Patient ID: patient identifier.

4.1.2. Characterization of lymphocytic and myeloid regulatory cellular subpopulations

In our previous study, we found that *HIV/STAT5B* and HIV/BACH2 chimeric transcripts were specifically enriched in regulatory T cells and central memory T cells (Tcm), while such enrichment was not found in T effector, T naïve, T stem cell memory (Tscm), T effector memory (Tem), total CD8+ T lymphocytes and monocytes [76]. Here, we examined whether the relative and absolute composition of other lymphocyte and myeloid cell populations having a regulatory function differed between the three groups of HIV-1 patients and healthy donors.

As depicted in Figure 4.1, no difference has been observed in the relative and absolute levels of CD4 T cells in PLWH (N=28) concerning healthy controls (HC), reflecting the good immunological status. According to inclusion criteria, subjects enrolled have to be on virological suppression under ART and with a good immunological profile (CD4 >500 cells/μL). On the other hand, the absolute count of CD8 T cells was higher among PLWH.

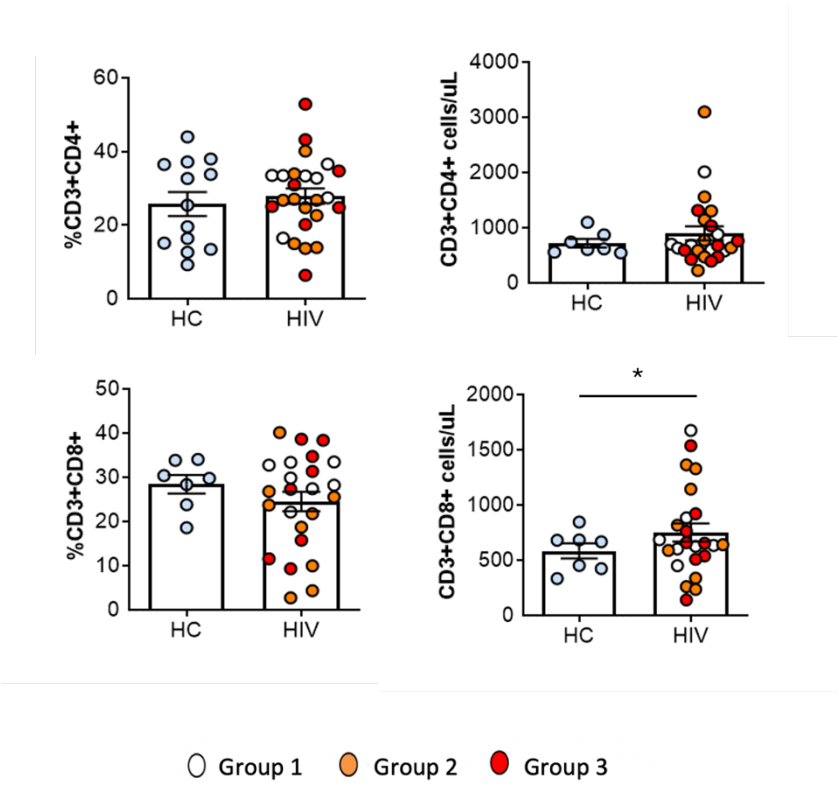


Figure 4.1. Characterization of the lymphoid compartment. Absolute and relative quantification expressed as cell/ul of the indicated cellular subtypes in healthy controls (HC) and in PLWH, subdivided for the 3 groups (Group 1 in white, Group 2 in orange and Group 3 in red). * p- value <0.05, as determined by Mann-Whitney test.

Moreover, the relative composition of naïve and memory T cell subsets was comparable between healthy controls (N=7) with respect to PLWH (N=24), as shown in Figure 4.2 and 4.3. Specifically, a significant reduction in the relative proportion within total CD8+ T cells of naive T cells was observed in PLWH, as depicted in Figure 4.3.

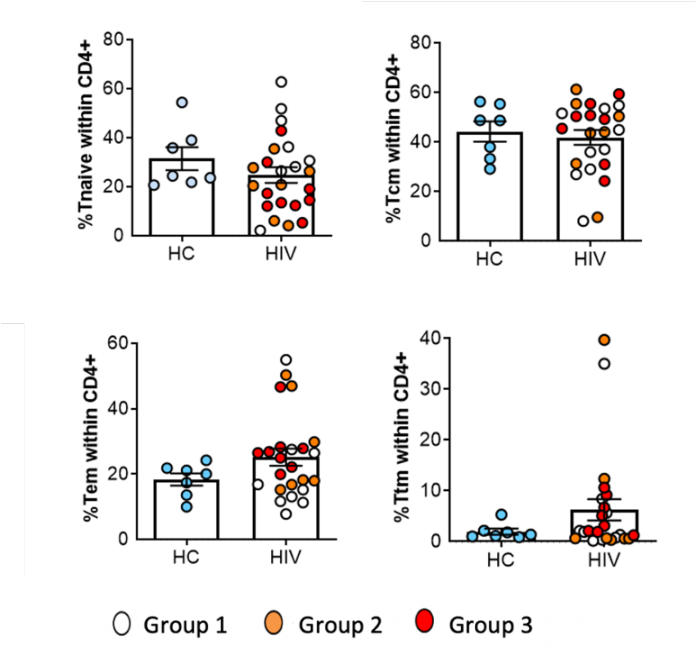


Figure 4.2. Characterization of the memory CD4+ T cells lymphoid compartment. Relative quantification of the indicated cellular subtypes.

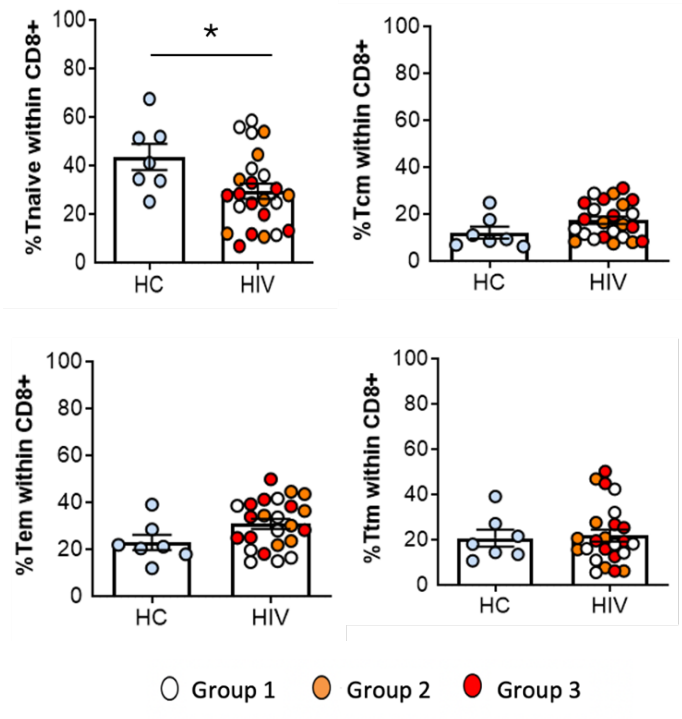


Figure 4.3. Characterization of the memory CD8+ T cells lymphoid compartment. A-D) Relative quantification of the indicated cellular subtypes. Statistical significance expressed as * p- value <0.05, as determined by Mann-Whitney test.

Concerning the regulatory compartment, we have investigated the composition of both the lymphocytic and the myeloid compartments in HC and in PLWH. Specifically, we tested 8 PLWH in Group 1, 11 in Group 2, and 9 in Group 3, while 16 healthy controls were included for comparison. We focused on classical FOXP3-expressing CD127-CD25+ Tregs and Tr1 cells, a subset of regulatory T cells characterized by their ability to secrete high levels of IL-10 without constitutive Foxp3 expression [91] (Figure 4.4) and found no significant differences between the two groups.

Additionally, two other types of regulatory T cells have been described: HLA-G+CD4+ T cells and HLA-G-specific CD8+ T cells. HLA-G, a tolerance molecule from the MHC inhibits CD4+ T-cell proliferation, induces long-term unresponsiveness in CD4+ T cells, and promotes the differentiation of T cells into immunosuppressive/regulatory T cells, such as CD4+HLA-G+ and CD8+HLA-G+ cells [139-141]. Notably, a significant increase in CD8+HLA-G+ T cells was observed in PLWH, which may be related to the abundance of the CD8+ T cells in this population (Figure 4.4) (data not shown).

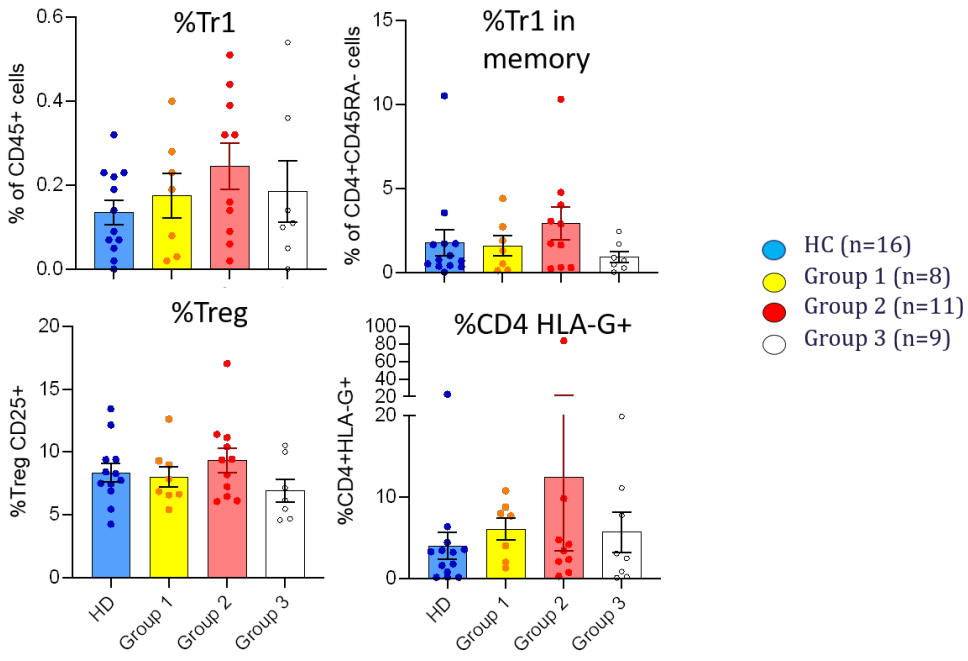


Figure 4.4. Characterization of the regulatory lymphoid compartment. Relative quantification of the indicated cellular subtypes. Statistical significance expressed as * p- value <0.05; ** p-value <0.01, as determined by Mann-Whitney test.

Next, we have characterized the regulatory myeloid compartment. The relative composition of 'classical' inflammatory monocytes (CD14highCD16−), 'intermediate' monocytes (CD14+CD16+) and 'non-classical' monocytes (CD14lowCD16+) is reported in Figure 4.5. The 'intermediate' and 'non-classical' monocytes have been shown to retain a regulatory function at the expense of a reduced phagocytic capacity (Figure 4.5) [98].

Additionally, the dendritic cells (DC) compartment, which consists of CD11c+ conventional DCs (cDC) expressing either CD1c (blood dendritic cell antigen-1, BDCA-1) or CD141 (BDCA3), and of CD11c-CD123+plasmacytoid DCs (pDCs) expressing BDCA-2, BDCA-4, and CD123 [109]. Specifically, DC identified as CD14- were classified into cDC1 if co-expressing CD11c and CD141 (BDCA-3) and as cDC2 when co-expressing CD11c e CD1c (BDCA-1) (Figure 4.5). Finally, we evaluated a particular subset of human tolerogenic DCs, termed DC-10, known for their ability to spontaneously secrete large amounts of IL-10 [110] (Figure 4.6) [142, 143].

No significant difference was found in the relative composition of these cellular subsets when compared between the different groups of PLWH and healthy donors.

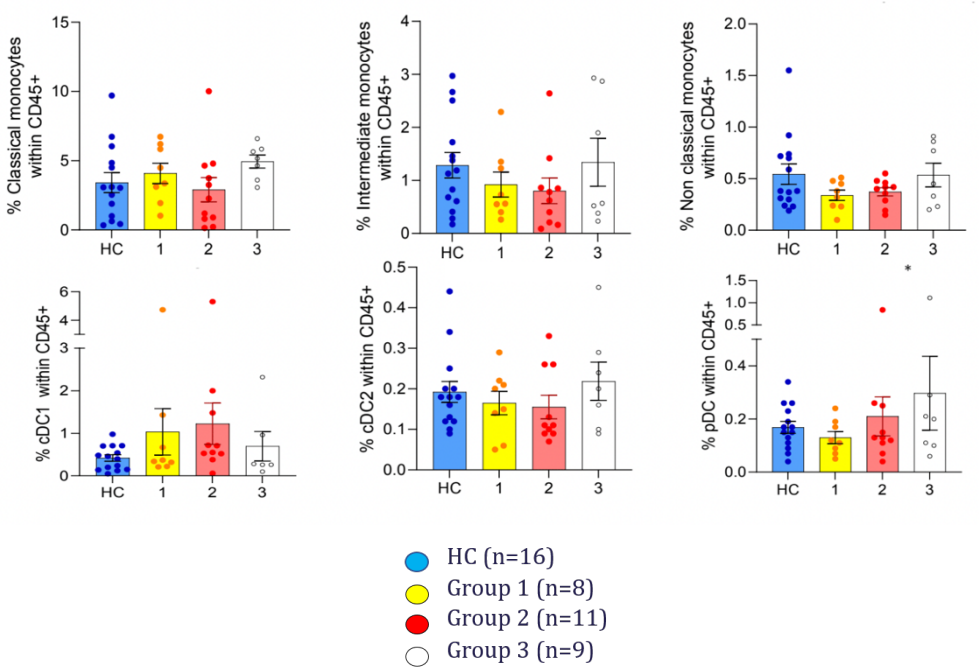


Figure 4.5. Characterization of the regulatory myeloid compartment. Relative quantification of the indicated cellular subtypes s in healthy controls (HC) and in PLWH. Statistical significance expressed as * p- value <0.05, as determined by Mann-Whitney test.

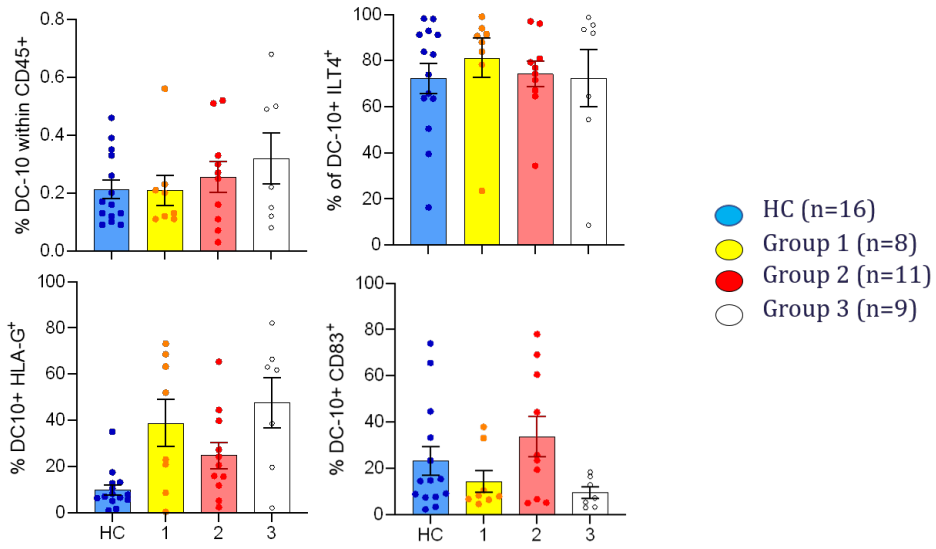


Figure 4.6. Characterization of the DC-10 compartment. Relative quantification of the indicated cellular subtypes s in healthy controls (HC) and in PLWH.

4.1.3. Quantification of intact and defective provirus

To assess the amount of intact and defective/hypermutated provirus copies, IPDA assay was performed on 24/28 individuals. L001, L002, L004 and L028 were excluded due to the limited amount of material available [44].

No differences were observed in the quantification of both intact and defective proviruses between those who initiated ART during CHI versus those who started in AHI, as assessed by Mann-Whitney non-parametric test. The graph below shows the medians for each group of patients, Figure 4.7. Since no significant differences were noted among the three groups, I have reported here the global median values for intact HIV-1 DNA (interquartile ranges, IQR) 48.43 (14.61- 225.81); for 5' deleted proviruses were 3,86 (0-117.29) and for 3' deleted 374.81 (162,53 - 653,54) copies/10^6 CD4 T cells.

Notably, L005 had zero copies of both intact and deleted provirus per 10^6 CD4+ T cells, despite being a subtype B. In contrast, L008 and L013 had undetectable levels of HIV-1 DNA and of defective 5' deleted proviruses, but detectable levels of 3' deleted proviruses

(359.9 vs 14.8 and 211.6 copies/10^6 CD4+ T cells, respectively). On the other hand, high levels of intact provirus were found in L004 and L011 (458.3 and 4649.1 copies/10^6 CD4+ T cells, respectively) with even higher amounts of defective proviruses.
Additionally, L007 and L022, belonging to Group 3, exhibited very high levels of intact DNA (151,140.68 and 16,231.29 copies/10^6 CD4+ T cells, respectively), resulting in negative results when calculating the amount of 5' and 3' deleted proviruses (data not reported in the graph).

The results show high variability among the groups and are in line with IPDA values reported in other HIV patient cohorts [45, 138] (Figure 4.7).

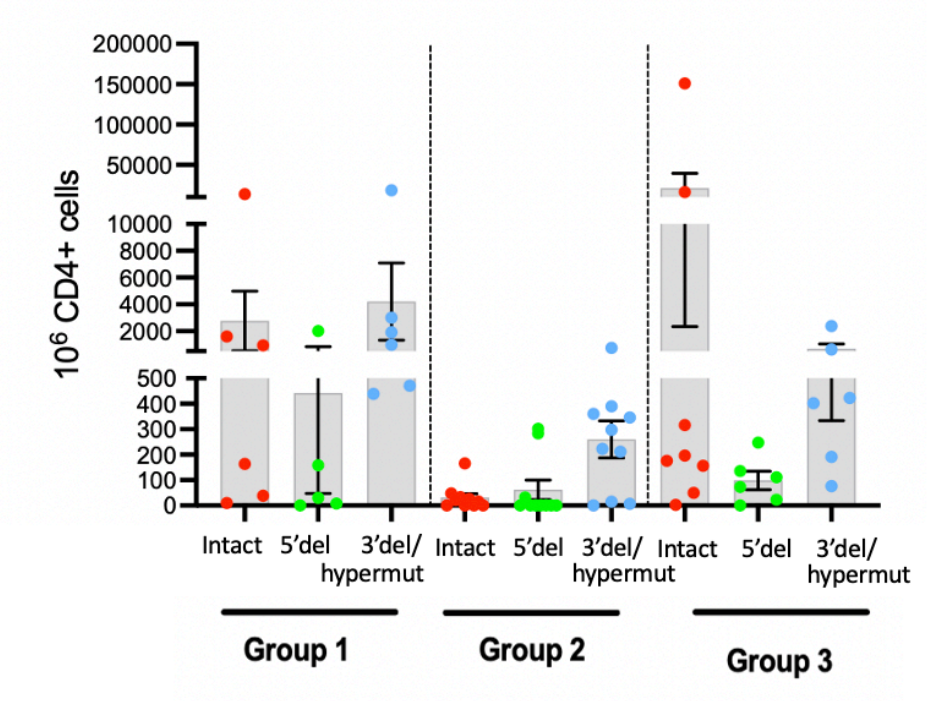


Figure 4.7. Quantification of intact and defective proviruses with deletion at 5' or at 3' 3'or hypermutation at 3' in PERSHIST study. Dots represent participants enrolled (N=24), subdivided for the 3 groups. Horizontal black lines indicate mean values, with standard deviation.

However, no correlation has been found between the values for intact proviral DNA and the following variables: CD4 count nadir and at enrollment, CD4/CD8 ratio at diagnosis and at enrollment or the composition of cells in the regulatory compartments, namely Treg, Tr1, CD4+HLA-G+ and CD8+HLA-G+ cells.

4.1.4. Identification of the integration sites

Viral integration sites (IS) were retrieved from genomic DNA isolated from CD4+ T cells by a sonication-based PCR protocols named as Sonication Linker Mediated PCR (SLiM-PCR) (Material and Methods section for details). As HIV-1 is a highly mutagenic virus and HIV replication is highly error-prone, the retrieval of IS may be compromised by mutations introduced at the viral LTR sequence. Therefore, patient-specific PCR primers annealing to LTR sequences were used for the retrieval of integration sites. Using this approach, we retrieved 4559 integration sites (IS) from CD4+ T cells purified from the enrolled patients. Notably, the number of IS recovered from the different patients in our cohort was very variable, ranging from zero in subjects L001, L012, L013 to 1259 IS in L003. As shown in Figure 4.8, the integration profile confirmed the natural tendency of HIV-1 to integrate according to the distribution of RefSeq genes, spanning across the entire transcriptional unit.

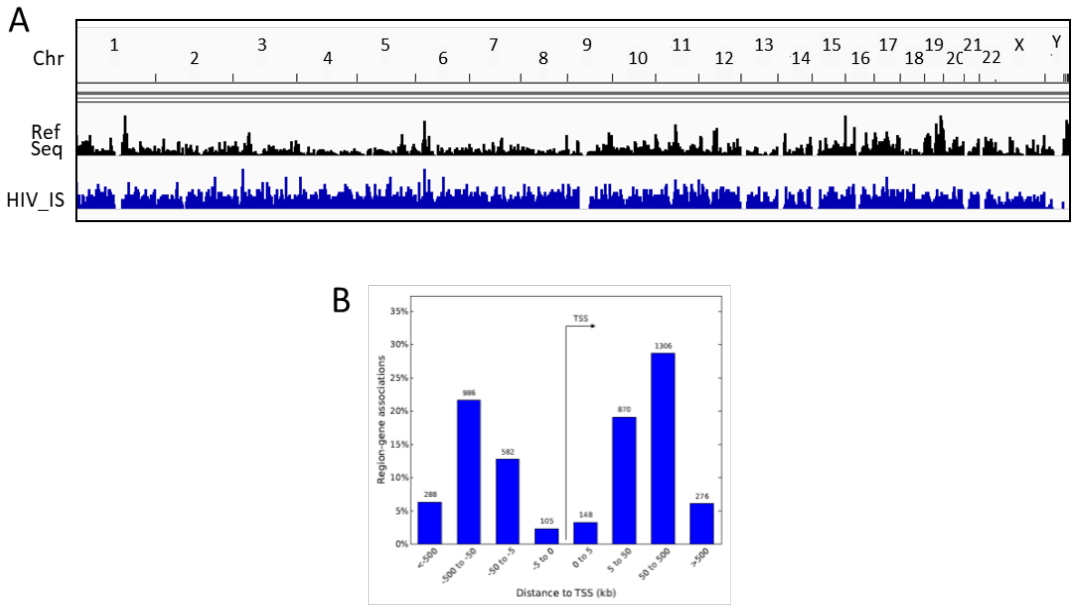
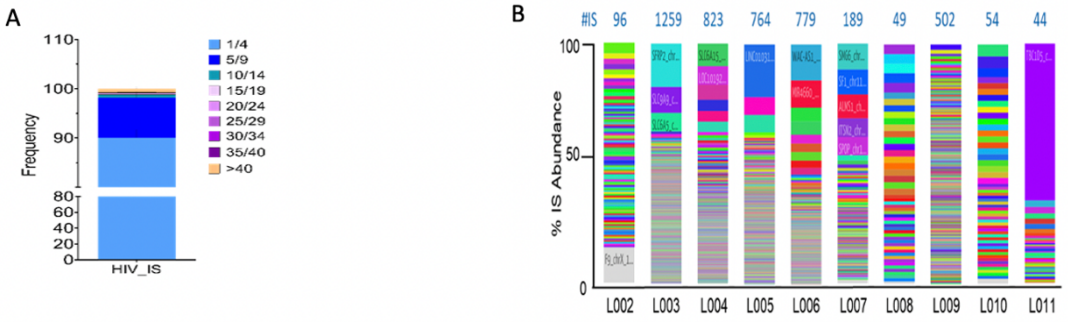


Figure 4.8. HIV-1 integration profile in the 13 enrolled subjects. A) Distribution of the viral integration sites of the 13 enrolled subjects (blue plot) in respect to the distribution of cellular genes displayed in the RefSeq (black plot). B-C) Distribution of IS in respect to the transcription start site (TSS) of HIV-1 (B).

Given that the SLiM-PCR technique relies on a physical fragmentation method of the genomic DNA (sonication) and molecular barcoding of the fragmented DNA occurred prior to PCR amplification, it is possible to accurately compute the clonal abundance of each IS. The assessment of clonal abundance is required to observe potential clonal expansions caused by insertional mutagenesis.

More than 90% ± 1.6 of the IS were represented by several genomes ranging from to 1 to 4, 8.2% ± 1.3 of the IS were represented by 5 to 9 cells, 0.6% ± 0.3 by 10 to 14 cells and the remaining 1,6% ± 0,43 by 15 to 400 cells (Figure 4.9). After estimating the number of genomes associated with each IS, we are able to infer the relative abundance of each IS as a percentage of the total IS identified in each sample. Overall, the relative abundance of HIV-infected clones was low, averaging 0.84% ± 0.3. However, in subjects L003, L005, L006 and L011 some clones displayed a high relative abundance, ranging from 7 to 65%, as reported in Figure 4.9. In this Figure, I listed the twelve most abundant IS, identified by the name of the closest cellular gene.



C

L002		L003		L004		L005		L006		L007		L008		L009		L010		L011	
Gene ID	%Rel.	Gene ID	%Rel.	Gene ID	%Rel.	Gene ID	%Rel.	Gene ID	%Rel.	Gene ID	%Rel.	Gene ID	%Rel.	Gene ID	%Rel.	Gene ID	%Rel.	Gene ID	%Rel.
P9	14.8	SFRP2	18.0	SLC6A15	9.4	LINC01031	21.9	WAC	14.9	SMG6	10.7	MIB2	4.0	LOC100505921	2.2	KMT2D	4.9	TBC1D5	65.2
SAMD4B	4.4	SLC9A9	10.8	LOC101927305	7.8	MIR4719	7.4	MIR4660	11.4	SF1	10.4	RBM14	4.0	PRUNE2	1.6	TMEM259	4.9	MGMT	2.7
C1orf159	2.2	SLC6A5	7.7	CNTNAP2	6.3	FDX1	7.3	CPEB2	5.7	ALMS1	9.9	GPS2	4.0	PBRM1	1.1	TICAM1	3.7	SRPK1	2.7
SLTM	2.2	LINC01309	1.1	LOXL1	4.7	ST6GALNAC5	1.2	SUCLG2	5.6	ITSN2	7.8	C3orf20	4.0	EHHADH	1.1	MACF1	2.5	SOX6	2.2
HEATR5B	2.2	VPS45	1.0	METTL4	4.4	CPLX2	1.1	LOC100996654	3.7	SPOP	7.6	ERI1	4.0	RSBN1	1.0	SLK	2.5	TMEM174	2.2
EXT1	2.2	TMEM132C	0.7	SPANXN1	4.4	KMT5B	0.7	FAM168A	3.6	CLN3	2.2	GNB1	2.7	PPP2R5A	0.8	ATL3	2.5	RIPK2	2.2
CTSS	1.5	FANCL	0.5	ADGRF5	1.3	PCDH9	0.5	ZNF385B	3.6	EHMT1	1.7	SKI	2.7	STAT5B	0.8	NUMB	2.5	LOC105369443	1.6
TPH1	1.5	LINC01828	0.5	ZNF407	1.1	CASC3	0.5	FUNDC2P2	3.0	USP9Y	1.7	USP48	2.7	SGSM3	0.8	GRB2	2.5	LOC100506022	1.1
LOC728084	1.5	GLDC	0.4	SLC25A32	1.1	SCAP	0.5	AUTS2	2.8	CCDC63	1.5	MCM10	2.7	ZFP69	0.6	GNA15	2.5	CLEC2D	1.1
URI1	1.5	CCDC155	0.3	LOC101928622	1.0	MROH1	0.5	LOC101927196	0.9	STAU2	1.2	LCOR	2.7	KRT5	0.6	USP40	2.5	CLIC4	0.5
LOC101929161	1.5	LRP2	0.3	SH2B1	1.0	STAT5B	0.4	LOC105369879	0.7	IQSEC1	1.0	PDCD11	2.7	TNRC6C	0.6	LINC01237	2.5	UCK2	0.5
C6orf48	1.5	GRIK2	0.3	TMEM175	1.0	ZSWIM5	0.4	LINC00977	0.7	ZZEF1	0.8	RGS10	2.7	LINC00971	0.6	GPCPD1	2.5	ERO1B	0.5

Figure 4.9. HIV-1 integration sites absolute (a) and relative (b) abundance, reporting the 12 most frequent is in the table (c), as identified by the nearest cellular genes.

Since the aim of the study was to identify potential hotspots for HIV-1 integration that may contribute to viral persistence, we focused on genes that frequently targeted by the virus. Among the 3349 unique targeted genes, only 265 were hit by at least two different

IS (7.9%), including genes such as KDM2A, GBE1, NF1, CDH8 and other genes known to be recurrently targeted by lentiviral vector integrations [145]. BACH2 (N=4), STAT5B (N=3) and MKL2 (N=4) were also identified to be targeted in our cohort of patients, thus confirming published results.

Additionally, to identify genes that may be activated through a promoter insertional mutagenesis mechanism, we examined the relative orientation of the integrated virus in relation to the targeted genes. HIV-1 virus integrated in the same transcriptional orientation as the cellular gene in 45% (n=120) of the 265 genes hit at least twice (Figure 4.10).

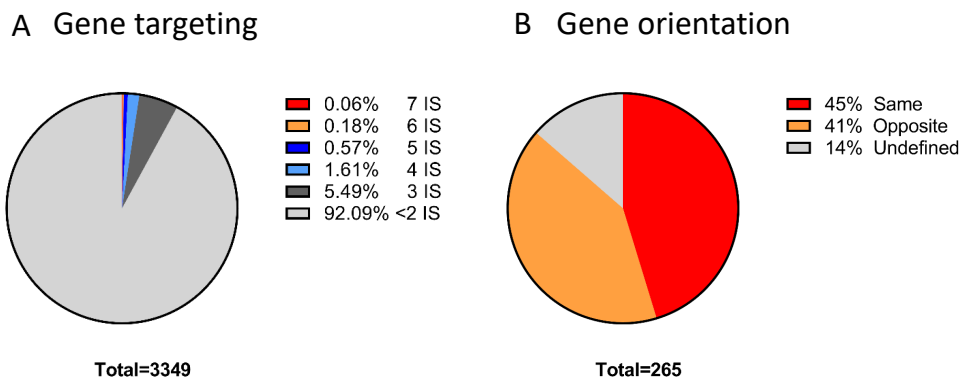


Figure 4.10. HIV-1 integration sites distribution withing genes (A) and by transcriptional orientation among 265 genes hit at least twice with the same IS (B).

4.1.4. Identification of the chimeric transcripts

By performing the previously described RT-PCR approach, we first assessed and evaluated the frequency of HIV/BACH2 and HIV/STAT5B chimeric transcript expressions in our cohort of patients. Overall, we found that 83% (N=11) of the 13 subjects enrolled expressed HIV/*STAT5B* transcripts, 38% (N=5) HIV/*BACH2,* and 31% (N=4) expressed both.

Group	ID	HIV/BACH2	HIV/STAT5B	%
1	L002	x	x	B: 50% S: 100%
	L004		x	
2	L005	x	x	B: 43% S: 85%
	L006		x	
	L008		x	
	L009	x		
	L010		x	
	L011	x	x	
	L013		x	
3	L001	x	x	B: 25% S: 75%
	L003		x	
	L007		x	
	L012			

Table 4.3. Detection frequency for the chimeric transcripts HIV/*STAT5B* and HIV/*BACH2* per patients and among the three groups.

Sequence analysis of the RT-PCR products revealed that the transcripts included the 5' HIV-1 LTR sequences, extending up to the canonical viral splice donor site, and were then accurately spliced to the first protein-coding exon of STAT5B in exon 2 and BACH2 in exon 6. No difference in the frequency or type of chimeric transcripts were observed among the three groups of patients analyzed, suggesting that the timing of treatment initiation and the duration of ART do not influence the rate and gene culprits implied in such mechanism of insertional mutagenesis (Table 4.3). These findings are consistent with those reported by Cesana et al., where no differences in the frequency of detection of HIV/STAT5B and HIV/BACH2 were observed among treatment-naïve [74].

1.2. IMMUNERaRe study

1.2.1. Characteristics of the cohort

Adult PLWH who started ART during PHI, defined as Fiebig stages I-V, on virological suppression under ART and with CD4+ T cell count > 350 cells/mm3 were enrolled. All these patients are in care at the Department of Infectious Diseases of IRCCS San Raffaele Institute (Milan, Italy).

Participants were stratified in three groups:

-Rapid Responders (RR), when CD4/CD8 ratio, absolute count of CD4+ and CD8+ T cells were within normal laboratory range within 8-12 weeks from cART initiation;

-Conventional Responders (CR), when CD4/CD8 ratio, absolute count of CD4+ and CD8+ T cells were within normal laboratory range after 12 weeks and within 48 weeks from cART initiation;
-Immunological non-Responders, when all three parameters were not normalized within 48 weeks.

Among 97 PLWH screened, 89 are considered for the analyses: 20 (22%) were classified as RR, 19 (21%) were CR and 50 (56%) as INR (Patients characteristics reported in Table 4.4). Participants were mostly male and median age at enrollment was 44.3 (36.4-52.6) years. Median days of ART start after diagnosis was 18.0 (10.0-31.0) with a median CD4 nadir of 494 (354-617) cell/μL and HIV-RNA at HIV diagnosis 166,578 (43,000 – 1,060,096) copies/mL.
All participants showed optimal immune-virological parameters at enrollment (Table 4.4).

Variable	Overall N=89	CR N=19	INR N=50	RR N=20	P value
Age	44.3 [36.4;52.6]	45.8 [37.3;53.9]	45.0 [36.9;52.2]	38.5 [35.2;52.5]	0.684
Male at birth	88 (98.9%)	19 (100%)	50 (100%)	19 (95.0%)	0.438
MSM	71 (79.8%)	14 (73.7%)	40 (80.0%)	17 (85.0%)	0.305
MSW/WSM	12 (13.5%)	4 (21.1%)	7 (14.0%)	1 (5.00%)	
Year of HIV diagnosis	2015 [2012;2017]	2015 [2012;2018]	2014 [2012;2016]	2016 [2014;2018]	0.226
Days to ART introduction	18.0 [10.0;31.0]	14.0 [7.00;40.5]	19.5 [12.0;27.8]	13.0 [9.50;29.5]	0.768
$CD4^+$ nadir (cells/mm^3)	494 [354;617]	459 [304;604]	467 [329;584]	585 [484;650]	0.142
Zenith VL (copies/mL)	166,578 [43,000; 1,060,096]	314,830 [89,513; 89,3766]	133,920 [29,274; 1,255,256]	166,578 [77,189; 309,121]	0.575
At HIV diagnosis					
CD4+ (cells/mm^3)	503 [366;650]	482 [304;604]	472 [337;647]	568 [496;658]	0.213
CD4%	22.9 [17.9;29.1]	22.6 [16.3;28.4]	21.4 [13.8;25.4]	29.4 [24.2;32.9]	0.004
CD8+ (cells/mm^3)	1164 [864;1685]	1164 [942;1528]	1258 [923;2046]	931 [677;1272]	0.065

CD8%	53.5 [46.2;63.1]	52.0 [42.7;63.6]	55.2 [50.5;64.6]	48.0 [39.4;51.5]	0.006
CD4/CD8 ratio	0.44 [0.27;0.62]	0.41 [0.24;0.68]	0.38 [0.18;0.53]	0.63 [0.51;0.90]	0.002
At screening					
CD4+ (cells/mm^3)	867 [656;1068]	906 [748;1094]	800 [634;1044]	992 [762;1070]	0.498
CD4%	37.6 [33.2;44.1]	40.2 [35.1;44.5]	35.1 [29.8;38.8]	45.2 [40.8;47.4]	<0.001
CD8+ (cells/mm^3)	711 [506;928]	638 [469;928]	803 [650;1005]	452 [354;590]	0.001
CD8%	31.5 [27.1;38.6]	27.3 [24.0;31.1]	37.4 [32.4;40.9]	25.5 [23.2;29.2]	<0.001
CD4/CD8 ratio	1.19 [0.87;1.59]	1.50 [1.21;1.80]	0.95 [0.74;1.21]	1.73 [1.47;1.93]	<0.001
Anchor drug class – NNRTI^	1 (1.12%)	0 (0.00%)	1 (2.00%)	0 (0.00%)	1.000
Anchor drug class – PI^	32 (36.0%)	8 (42.1%)	19 (38.0%)	5 (25.0%)	0.485
Anchor drug class – INSTI^	56 (62.9%)	11 (57.9%)	28 (56.0%)	17 (85.0%)	0.067

Table 4.4. Overall participants' characteristics stratified for each group.

Of note, 19/20 RR patients maintained the 3 immunological parameters within normal range for ≥ 4years, whereas among INR only 18/50 recovered CD4/CD8 ratio after > 48 weeks.

4.2.2. Characterization of putative predictive biomarkers: HLA class I-Killer-cell Immunoglobulin-like Receptor (KIR) matching

The receptors of the KIR family regulate the activation of NK cells through interaction with HLA -class I molecules. The genetic loci of KIR and HLA are highly polymorphic, and several studies have shown how certain HLA/KIR combinations act as a protective factor against viral infections. Indeed, the combination of KIRs and HLA gene/alleles is able to predict the outcome of viral infection Indeed, Malnati et al demonstrated that a complex Chromosome 6 haplotype that combined the presence of both HLA-Bw4-I80 expressing alleles and HLA-C2 escaping miRNA148a regulation (C2 High Alleles) is a distinctive feature of HIV infected individuals that naturally control HIV-1 viremia (elite

controllers) [146]. Therefore, in order to identify predictive biomarkers of immunological control, the HLA class I - KIR matching was studied.

In collaboration with Dr. Malnati (Viral Evolution and transmission Unit) and Dr. Chimienti (Diabetes Research Institute) we first evaluated the proportion of the protective haplotypes containing high-expression HLA-C2 alleles, with and without HLA-B Bw4-Isoleucine80 (I80) (Figure 4.11), without identifying significant enrichment in any group. Conversely, the proportion of functional pairs between these protective HLA alleles and their activating KIR counterparts was significantly enriched ($p< 0.01$) in RR compared to INR (Figure 4.12). This finding highlights an interesting parallel with EC, who exhibit a genotype indicative of epistasis between activating KIRs and their HLA-B and -C2 ligands [146].

Noteworthy, when we assessed the balance between the activating (aKIR) and inhibitory (iKIR) KIR within each group we found a striking difference. As shown in Figure 4.13, RR displayed a >20% higher proportion of functional aKIR/HLA pairs compared to iKIR ones, whereas INR exhibited a great predominance of iKIR. This imbalance may contribute to a significantly higher capability of NK cells to recognize and eliminate infected cells in the RR group.

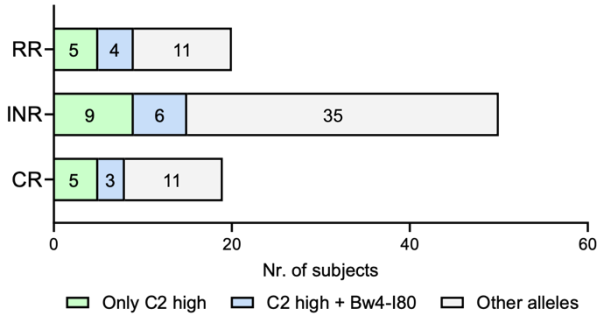


Figure 4.11. Proportion of PLWH with the protective haplotypes containing high-expression HLA-C2 alleles, with and without HLA-B Bw4-Isoleucine80 (I80), among the three groups.

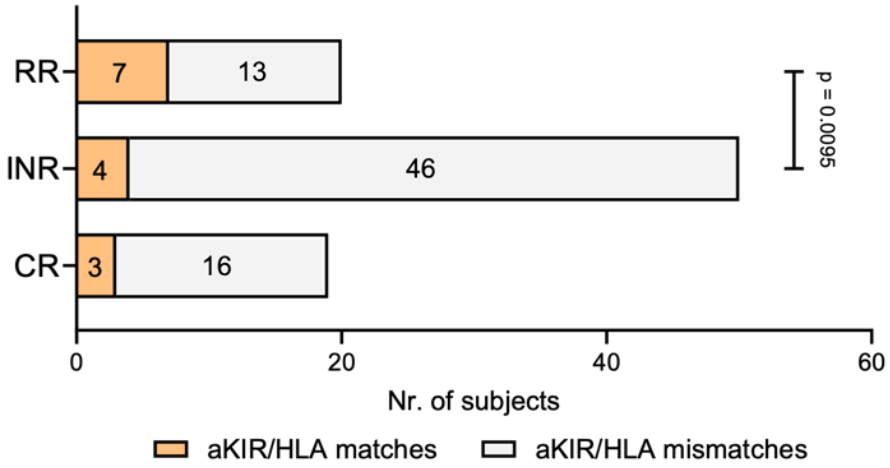


Figure 4.12. Proportion of PLWH with matches and mismatches of functional pairs between protective alleles and their activating KIR counterparts.

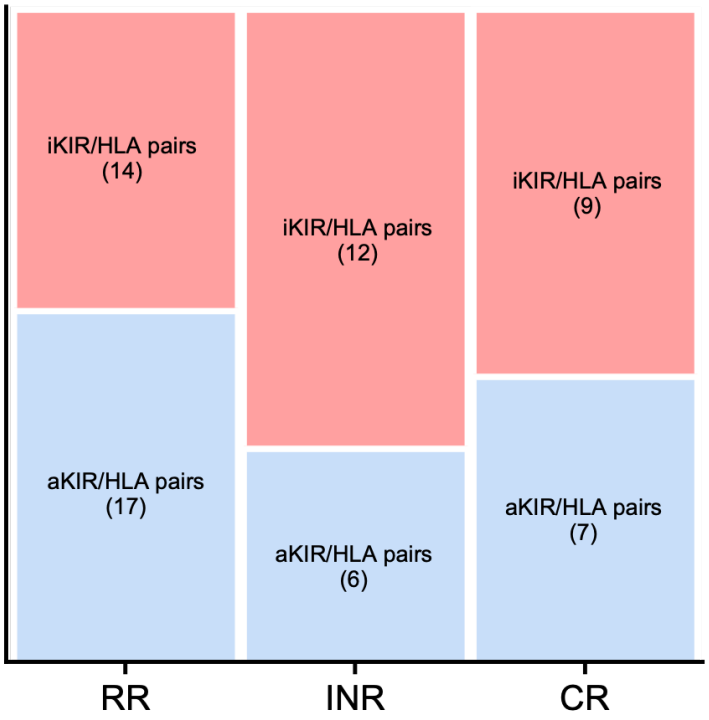


Figure 4.13. Proportion of PLWH with activating (aKIR) and inhibitory (iKIR) KIR within each group.

4.2.3. Quantification of intact provirus

To assess the amount of intact and defective/hypermutated provirus copies, IPDA assay was performed on 87/89 subjects [44]; the analysis was withheld for two individuals (RARE048, RARE 074) due to technical issues.

To perform the analysis, CD4+ T cells were purified, achieving an overall purity of over 80%. Notably, 51/89 HIV-1 genotypes were subtype B, while 21/89 were unknown and 16/89 belonged to other clades/recombinant viruses, which could represent a potential limitation to the method used.

Quantification of both intact and defective proviruses was similar among the 3 groups, as assessed by Mann-Whitney non-parametric test (Figure 4.14). Specifically, the overall median for intact HIV-1 DNA was 116.38 (interquartile ranges, IQR; 0.00-463.57); for 5' deleted proviruses it was 426.82 (109.27-895.7) and for 3' deleted proviruses it was 641.35 (126.92 - 1493.03) copies/10^6 CD4 T cells.

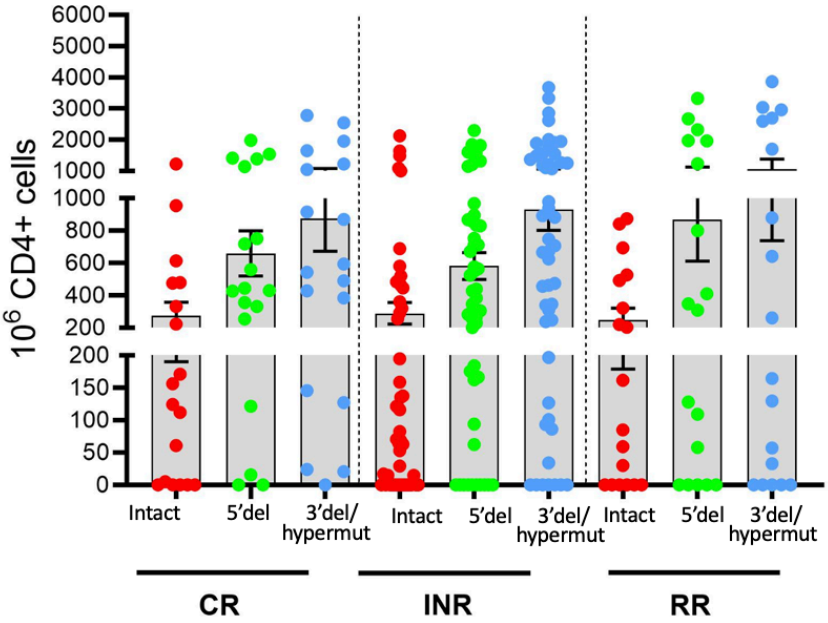


Figure 4.14. Quantification of intact and defective proviruses with deletion at 5' or at 3'or hypermutation at 3' in IMMUNERaRe study. Dots represent enrolled PLWH (N=86), subdivided for the 3 groups. Horizontal black lines indicate mean values, with standard deviation.

4.3. Intact proviral HIV-1 DNA in acute and chronic HIV infection

To further quantify the viral reservoir in people who started ART in AHI and CHI, we compared the results obtained from the IMMUNERaRe and PERSHIST studies. After excluding participants from Group 3, we compared the IPDA results for the two cohorts. We found that intact HIV-1 DNA levels were significantly lower in participants enrolled in the IMMUNERaRe (those who started ART at AHI) compared to those in the PERSHIST study (p: 0.042). On the other hand, defective proviruses with deletions at 5' were significantly higher in the IMMUNERaRe cohort (p: 001), suggesting that HIV may not have yet fully established stable and functional reservoirs when ART is administered early in acute infection.

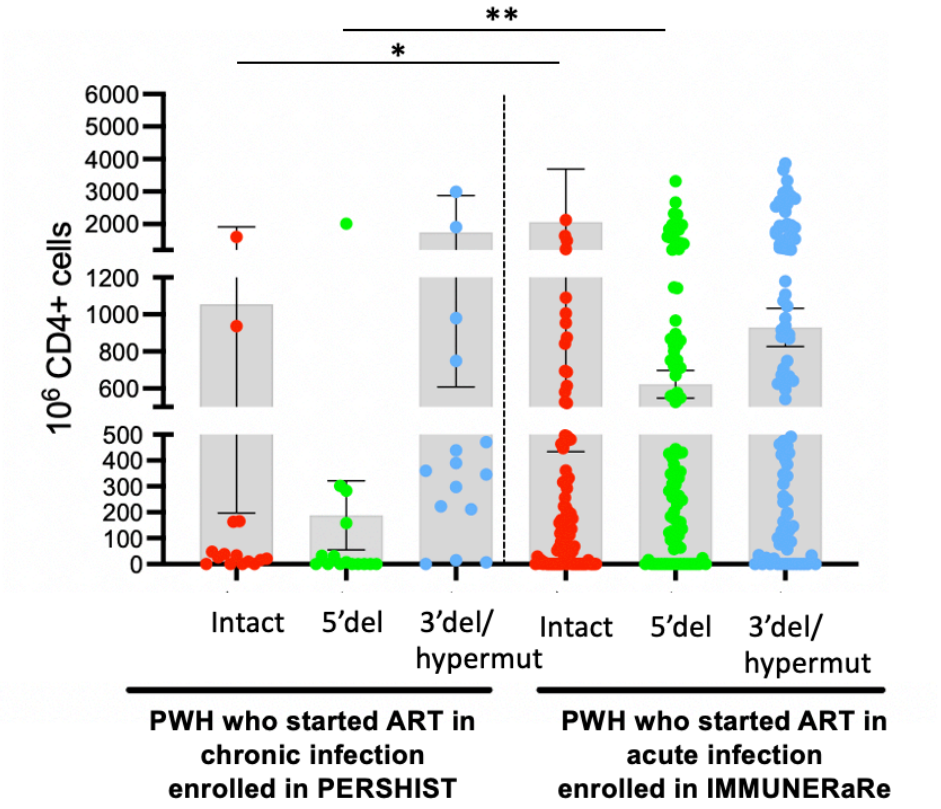


Figure 4.15. Quantification of intact and defective proviruses with deletion at 5' or at 3' 3'or hypermutation at 3' in PERSHIST study who started ART in CHI (N=16) and PLWH enrolled in IMMUNERaRe study who started ART in AHI (N=86). Dots represent participants enrolled. Horizontal gray lines indicate mean values, with standard deviation.

6. DISCUSSION

The existence of an HIV reservoir and its persistence pose significant challenges to viral eradication. Thus, it is essential to explore, identify, and understand the mechanisms behind its persistence, as these could represent potential therapeutic targets.

In this study, we characterized the regulatory compartment of T cell lineages in HIV-infected individuals who began treatment during either the acute or chronic phase. As shown, FOXP3-expressing Treg cells play a role in promoting viral persistence in PLWH undergoing suppressive ART. Specifically, we identified the expression of chimeric transcripts between the viral genome and adjacent cellular genes, such as BACH2 and STAT5B, produced as a result of insertional mutagenesis in Tregs and T central memory cells. Treg cells are a distinct subset of lymphocytes crucial for maintaining immune tolerance through their immunosuppressive functions. Due to their ability to harbor and sustain viral persistence, they have been proposed as a cellular reservoir for HIV. It has been demonstrated that Tregs contain a higher amount of HIV DNA compared to other T cell subsets [147, 148], can produce infectious viral particles upon activation, and the impaired IL-2 production seen during active HIV infection may promote post-integration viral latency, resulting in anergy [149]. Based on these findings, and considering the regulatory compartment's role in modulating immune system activity [124, 125], we aimed to investigate whether other regulatory cells, such as non-classical Tregs (Tr1), DC-10, and HLA-G expressing cells, might also contribute to supporting viral persistence.

It has been demonstrated that HIV-exposed DCs adopt a more tolerogenic phenotype [136], and that monocytes expressing HLA-G are more prevalent among PLWH on ART compared to untreated patients [135]. However, the role of DC-10 cells in HIV-1 infection has not yet been investigated. Consistent with our findings, previous studies have shown an increased relative proportion of CD8+HLA-G+ cells within the total CD8 T-cell population in PLWH, particularly those with controlled HIV-1 infection, with an inverse relationship between the proportion of HLA-G+ HIV-1-specific CD8 cells and viral load [150, 151]. Furthermore, the relative and absolute proportions of HLA-G-expressing CD4 T cells were found to be lowest in HIV-1 progressors [152]. Unlike conventional Tregs, Tr1-like cells have been shown to reduce immune activation without suppressing effector Th1 responses during acute HIV infection. These cells play a critical role in regulating

the inflammatory response, especially at peripheral mucosal sites, where HIV replication primarily occurs [96]. To investigate this further, we examined the absolute and relative composition of different regulatory T cell subpopulations in our cohort of PLWH, including subjects who began therapy during the acute and chronic phases, and compared them with age-matched healthy donor controls. Our results suggest no significant differences in the frequency of FoxP3-expressing Tregs, Tr1, or DC-10 regulatory cells among PLWH with good immunological status and controlled viremia, as compared to non-infected individuals. A notable increase in HLA-G-expressing CD8+ cells was observed in PLWH compared to healthy controls. However, these differences may be attributed to the overall increase in the frequency and absolute number of CD8+ cells. Due to the limited sample size in our cohort, no definitive conclusions can be drawn across the three groups.

Molecular analyses revealed the presence of HIV/BACH2 and HIV/STAT5B chimeric transcripts in our cohort of PLWH, confirming previous results. The frequency of these chimeric transcripts was similar in the three groups of PLWH, suggesting that the timing of treatment initiation and the duration of ART do not impact on the rate of insertional mutagenesis or on the gene targeting. Consistently, the regimen of cART (NNRTI vs NRTI) was found not to influence the frequency of HIV/STAT5B and HIV/BACH2 [76].

We retrieved 4559 HIV integration sites from our cohort of HIV patients. A high level of variability in the efficiency of IS retrieval was observed among subjects as we have zero IS for subjects L001, L012, L013 up to a maximum of 1259 IS in L003. Interestingly, two of the subjects, L001 and L012 belong to the group of patients who introduced ART in AHI. Among L001-L013, no correlation was seen between the number of IS retrieved and the amount of HIV DNA quantified by ddPCR. This result can be justified by the fact that the HIV region tested by different molecular assays is different and the presence of mutations within the HIV sequence may impact on the efficiency of retrieval of IS as well as in the quantification of the amount of HIV-DNA.

However, the reliability of our integration study was demonstrated by the typical preference of HIV IS in targeting the transcriptional unit of Ref Seq genes. Morevoer, in agreement with published results, also in our cohort of HIV subjects that received ART in acute and chronic infections BACH2, STAT5B and MKL2 were among the most frequently targeted genes. Other genes, such as KDM2A, GBE1, NF1, CDH8, were also

found to be targeted by different IS. However, they were never described as culprits of insertional mutagenesis in PLWH; instead, they are frequently targeted by vector insertion as a consequence of an integration bias and not as the results of a selective process occurring in hematopoietic cells [145].

The majority of HIV IS were represented by a limited number of cells, indicating that the majority of circulating clones did not significantly expand. However, in subjects L003, L005, L006 and L011 clones represented by a higher number of fragments and corresponding to a high relative abundance, rising to 65%, were detected. The analyses of IS from a single timepoints analyzed did not allow us to define if these abundant IS came as the results of insertional mutagenesis events that will progressively expand or the sporadic fluctuation of infected cell clones in response to homeostatic or antigenic stimuli. As shown in longitudinal studies of integration site analyses in patients under ART, the abundance of clones with the insertional mutagenesis events was low, averaging 2.3% of the total number of HIV-infected clones [24, 62]. However, it should progressively increase over time. On the contrary, infected cells that wax and wane following the dynamics of the adaptive immune response may achieve high levels of abundance and shrink within a short period of time. Hence, it would be interesting to perform longitudinal integration studies to assess the recovering and abundance of the same clones over time.

A better approach for the identification of novel putative culprits that may favor the persistence of the HIV reservoir is the retrieval of chimeric transcripts. The evidence that this mechanism can promote the activation of other genes than BACH2 and STAT5B providing a selective advantage and possibly leading to neoplastic transformation has been provided by a recent work published by Mellors and colleagues. In this work, proviral integrations targeting the signal transducer and activator of transcription 3 (STAT3) and lymphocyte-specific protein tyrosine kinase (LCK) genes have been identified in T-cell lymphoma that occurred in people with HIV-1 infection [153]. As seen for BACH2 and STAT5B, viral integrations were in the same transcriptional orientation of the targeted genes and led to the activation of those genes by insertional mutagenesis mechanisms. With our work we have provided evidence that the identification of HIV chimeric transcripts from cellular RNA is much more efficient than the retrieval of integration sites. Indeed, although HIV integrations in BACH2 and

STAT5B were identified in 3 patients of our cohort, all subjects apart from one were positive for HIV/BACH2 and HIV/STAT5B chimeric transcripts by RT-PCR.

For this reason, we are currently developing in the lab a PCR protocols that would allow the retrieval of chimeric transcripts that can originate between the integrated virus and the nearby cellular gene in a high-throuput fashion. The new method, referred as Chim-seq PCR is based on the protocol published by Picelli and colleagues [154, 155], according to which the coding RNA (polyA) is retrotranscribed into double-stranded and full-length cDNA, tagmented by a hyperactive derivative of the transposase Tn5 and ligated to specific linker cassettes allowing the amplification and sequencing of the library obtained. We modify the protocols in order to specifically amplify the chimeric transcript that may occur between the integrated HIV genome and the surrounding cellular gene. Thanks to this approach, we will be able to identify if chimeric transcripts will be produced in the different T cell subsets and regulatory cell.

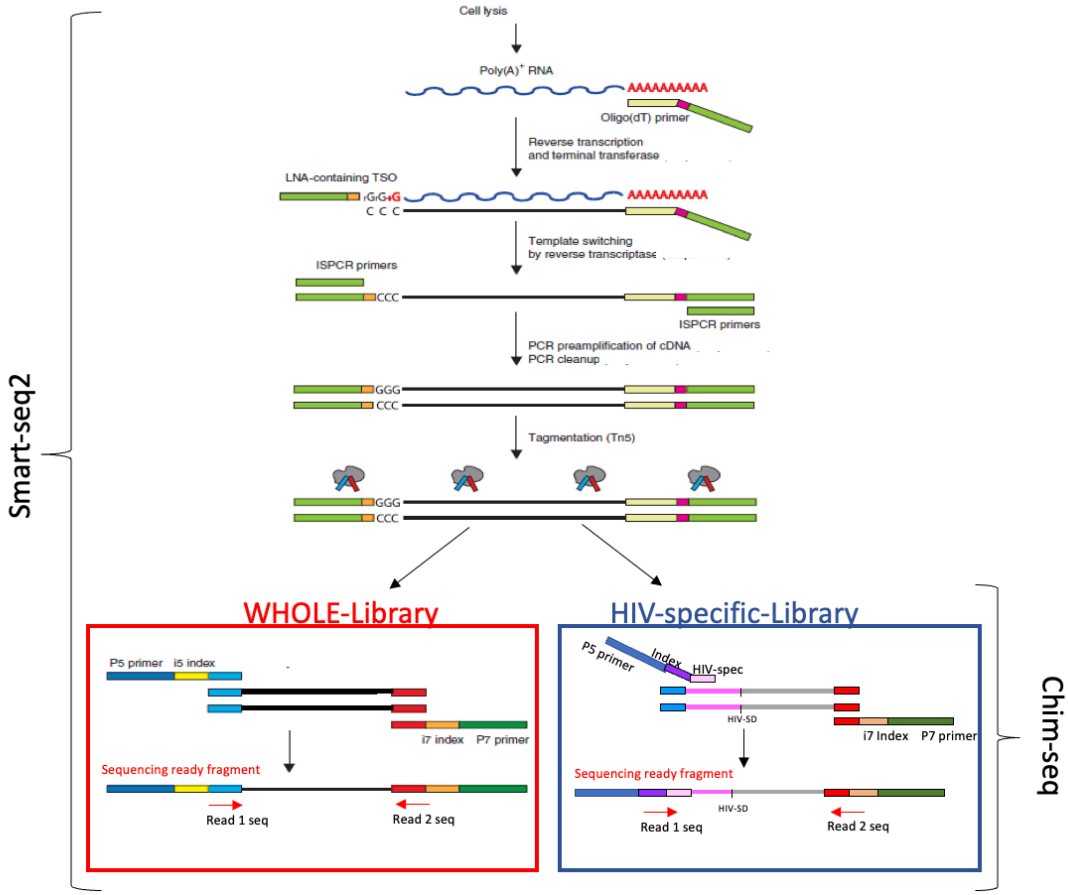


Figure 5.1. Schematic representation of the Chim-seq strategy to be employed to retrieve chimeric transcripts, specifically amplifying those originating between the integrated HIV genome and the surrounding cellular gene.

Finally, we characterized the reservoir in PLWH who initiated ART during AHI and CHI. Our data reveal significant variability, both in the PERSHIST and in the IMMUNERaRe studies, consistent with previous studies in different cohorts, including PLWH with viruses resistant to the four major classes of antiretrovirals [45, 138, 156]. Specifically, we found that PLWH who initiated ART during AHI enrolled in IMMUNERaRe had lower amount of intact HIV-1 DNA compared to those who started ART during CHI enrolled in PERSHIST. This finding is consistent with observations in previous cohorts [29, 39, 157], where HIV reservoir is smaller in PLWH treated in AHI. However, this contrasts with a similar study conducted in a cohort of PLWH who began ART in early Fiebig stages, where a lower amount of total HIV-DNA was noted, but no differences were found in intact HIV DNA or outgrowth of virus [158]. Also in longitudinal studies, levels of intact virus were found to be higher in individuals who started ART during AHI, as compared to those treated during CHI [159]. In the context of the study, this discrepancy could be explained by higher initial levels of intact DNA in AHI individuals compared to those treated in CHI, with selective decay over longer ART suppression times. Indeed, in the study by Falcinelli et al., mean time to sampling was of 0.81 years of viral suppression with ART. Conversely, in our cohort, the median time on ART at sampling was greater than 5 years. According to a mathematical model, the decay of intact and defective HIV DNA follows a rapid and biphasic pattern, with an initial rapid decay of intact HIV DNA at a half-life (t1/2) of approximately 2.83 years, followed by a slower second phase with a t1/2 of about 15.4 weeks (~3.9 months) [160].
In this work, we found a significantly higher amount of defective proviruses with deletions at 5' region, in PLWH treated in AHI. Indeed, defective proviruses accumulate quickly during AHI [161]. This suggests that when ART is initiated early during acute HIV infection, the virus may not have had sufficient time to fully establish stable and functional reservoirs.

PLWH who started ART in acute infection were further characterized in the context of the IMMUNERaRe study in order to identify predictive biomarkers of immunological control. The most comprehensive evaluation of PTC comes from the French VISCONTI cohort, which included 14 individuals [162], from the CASCADE collaboration, the SPARTAC trial and from the Control of HIV after Antiretroviral Medication Pause

(CHAMP) study, which reports 67 PTCs through 14 studies encompassing treatment interruption [163-165, 17]. PTCs rarely carry the so-called "protective" HLA alleles, which are overrepresented in EC and LTNP and are associated with enhanced immune control of HIV replication [164, 166-168]. These protective HLA class I alleles, such as HLA-B^57, HLA-B^27, and HLA-B^58:01, have been widely reported to confer a stronger CTL response against HIV, leading to lower viral loads and delayed disease progression in ECs and LTNPs [169-172]. However, the immune control observed in PTCs appears to be largely independent of these classical protective HLA alleles, suggesting alternative mechanisms may be at play in maintaining post-treatment viral suppression. Previous reports suggest that NK cell responses are modulated by HLA-KIR interactions, influencing the trajectory of viral infections, including HIV [146, 173], and of immune control in different patient populations, including transplant patients [174].
To further investigate immune control mechanisms in PTCs, we analyzed the interactions between HLA class I molecules and their corresponding KIRs on NK cells, a key component of innate immunity. Our findings revealed that the proportion of functional HLA-KIR pairs, specifically those involving aKIRs and protective HLA alleles, was significantly enriched in RR, as compared to INR. In particular, RR exhibited more than 20% higher proportion of functional aKIRs relative to iKIRs. On the other hand, INR displayed a marked predominance of iKIRs. Previous studies have shown that a complex genotype characterized by high expression of HLA-C alleles from the C2 group and their corresponding KIR 2DS receptor ligands is a distinguishing feature of the EC, but not of long-term non-progressors. Specifically, EC with a complete KIR B haplotype, which includes both 3DS1 and multiple 2DS genes, along with their specific HLA-B and -C ligands, may be better equipped to overcome KIR-mediated inhibitory signals. This, in turn, could facilitate the direct recognition and more rapid clearance of HIV-infected cells. [146]. This imbalance may have profound implications for NK cell function in INR individuals. The dominance of iKIR interactions in INR may contribute to reduced NK cell-mediated immune surveillance, thereby facilitating immune evasion by the virus and promoting viral persistence.

Limitations of the study are the small sample size of the PERSHIST cohort, forced by the very material-, labor- and cost-demanding technique of integration analysis. The small

sample size may have also limited the immunophenotypic characterization of the regulatory compartment, and the IPDA results might not show significant differences across the various HIV groups. Clonal analysis was performed at a single time point, limiting the detection of integration site and the longitudinal study of the behaviour of such infected clones. Further molecular studies on mRNA collected from the different T cell subsets will provide insights on other putative culprits of viral persistence. On the other hand, In the IMMUNERaRe study, a single timepoint was collected for analysis, which makes it challenging to determine whether the immune responses observed are associated with ongoing stimulation.

7. CONCLUSIONS

Our study provides valuable insights into the intricate mechanisms underlying HIV persistence and immunological control in PLWH. However, several questions are still unanswered. Indeed, the processes of antigen-driven clonal expansion and selection contribute to the enduring maintenance and proliferation of HIV-1–infected clones, making eradication efforts more challenging. As a result, a deeper understanding of mechanisms HIV persistence is essential for the development of novel therapeutic targets that could provide strategies for eradication of the HIV reservoir. Further research is also necessary to assess whether enhancing aKIR-mediated activation could offer a promising approach to improving immune control. The ATI phase of the IMMUNERaRe study may provide valuable insights to support this hypothesis.

BIBLIOGRAPHY

1. Centers for Disease, C., Pneumocystis pneumonia--Los Angeles. MMWR Morb Mortal Wkly Rep, 1981. 30(21): p. 250-2.
2. Barre-Sinoussi, F., et al., Isolation of a T-lymphotropic retrovirus from a patient at risk for acquired immune deficiency syndrome (AIDS). Science, 1983. 220(4599): 868-71.
3. Consolidated Guidelines on HIV Prevention, Diagnosis, Treatment and Care for Key Populations - 2016 Update. 2016: Geneva.

4. Campbell-Yesufu, O.T. and R.T. Gandhi, Update on human immunodeficiency virus (HIV)-2 infection. Clin Infect Dis, 2011. 52(6): 780-7.
5. Hemelaar, J., The origin and diversity of the HIV-1 pandemic. Trends Mol Med, 2012. 18(3): 182-92
6. Perelson, A.S., et al., Decay characteristics of HIV-1-infected compartments during combination therapy. Nature, 1997. 387(6629): p. 188-91.
7. Cillo, A.R. and J.W. Mellors, Which therapeutic strategy will achieve a cure for HIV-1? Curr Opin Virol, 2016. 18: p. 14-9.
8. Hutter, G., et al., Long-term control of HIV by CCR5 Delta32/Delta32 stem-cell transplantation. N Engl J Med, 2009. 360(7): p. 692-8.
9. Gupta RK, et al. Evidence for HIV-1 cure after CCR5Δ32/Δ32 allogeneic ha<Seattle, Washington. 2019. Analytic treatment interruption (ATI) after allogeneic CCR5-D32 HSCT for AML in 2013.
10. Jensen B.O., Knops E., Lübke N. Conference on retroviruses and opportunistic infections. Seattle, Washington. 2019. Analytic treatment interruption (ATI) after allogeneic CCR5-D32 HSCT for AML in 2013.
11. Dickter J, et al. The 'City of Hope' Patient: Prolonged HIV-1 Remission Without Antiretrovirals (ART) After Allogeneic Hematopoietic Stem Cell Transplantation (aHCT) of CCR5-Δ32/Δ32 Donor Cells for Acute Myelogenous Leukemia (AML). Late Breaker B Abstract 12508. Presented at the 24th International AIDS Conference, July 29 – August 2, 2022.
12. Hsu J et al. HIV-1 remission with CCR5Δ32Δ32 haplo-cord transplant in a U.S . women: IMPAACT P1107. Conference on Retroviruses and Opportunistic Infections, abstract 65LB, 2022.
13. Teleshova, N., et al., Simian immunodeficiency virus interactions with macaque dendritic cells. Adv Exp Med Biol, 2013. 762: 155-81.
14. Hu, J., et al. Simian immunodeficiency virus rapidly penetrates the cervicovaginal mucosa after intravaginal inoculation and infects intraepithelial dendritic cells. J Virol, 2000. 74(13): 6087-95.
15. Clapham, P.R. and A. McKnight., HIV-1 receptors and cell tropism. Br Med Bull, 2001. 58: 43-59.

16. Fiebig, E.W., et al., Dynamics of HIV viremia and antibody seroconversion in plasma donors: implications for diagnosis and staging of primary HIV infection. AIDS, 2003. 17(13): 1871-9.
17. Namazi, G. et al. The control of HIV after antiretroviral medication pause (CHAMP) study: Posttreatment controllers identified from 14 clinical studies. J. Infect. Dis. 218, 1954–1963 (2018).
18. Boulassel, M.R., et al., CD4 T cell nadir independently predicts the magnitude of the HIV reservoir after prolonged suppressive antiretroviral therapy. J Clin Virol, 2012. 53(1): 29-32.
19. Ho, D.D., et al., Rapid turnover of plasma virions and CD4 lymphocytes in HIV-1 infection. Nature, 1995. 373(6510): 123-6.
20. Gelderblom, H.R., M. Ozel, and G. Pauli, Morphogenesis and morphology of HIV. Structure-function relations. Arch Virol, 1989. 106(1-2): 1-13.
21. Wu, Y., HIV-1 gene expression: lessons from provirus and non-integrated DNA. Retrovirology, 2004. 1: 13.
22. Craigie, R. and F.D. Bushman, HIV DNA integration. Cold Spring Harb Perspect Med, 2012. 2(7): a006890.
23. Singh, P.K., et al. LEDGF/p75 interacts with mRNA splicing factors and targets HIV-1 integration to highly spliced genes. Genes Dev, 2015. 29(21):228-797.
24. Maldarelli, F., et al. HIV latency. Specific HIV integration sites are linked to clonal expansion and persistence of infected cells. Science, 2014. 345(6193):179–83.
25. Coffin, J.M., et al. Integration in oncogenes plays only a minor role in determining the in vivo distribution of HIV integration sites before or during suppressive antiretroviral therapy. PLOS ONE, 2021.
26. Serrao, E., et al., Key determinants of target DNA recognition by retroviral intasomes. Retrovirology, 2015. 12: 39.
27. Wu, X., Burgess SM. Integration target site selection for retroviruses and transposable elements. Cell Mol Life Sci, 2004. 61(19–20):2588–96
28. Eisele, E. and R.F. Siliciano, Redefining the viral reservoirs that prevent HIV-1 eradication. Immunity, 2012. 37(3): 377-88.

29. Chun, T.W., et al., Early establishment of a pool of latently infected, resting CD4(+) T cells during primary HIV-1 infection. Proc Natl Acad Sci U S A, 1998. 95(15): 8869-73.
30. Ananworanich J., et al; RV217 and RV254/SEARCH010 study groups, HIV DNA Set Point is Rapidly Established in Acute HIV Infection and Dramatically Reduced by Early ART. EBioMedicine, 2016. 11:68-72.
31. Ho, Y.C., et al., Replication-competent noninduced proviruses in the latent reservoir increase barrier to HIV-1 cure. Cell, 2013. 155(3): 540-51.
32. Lorenzo-Redondo, R., et al., Persistent HIV-1 replication maintains the tissue reservoir during therapy. Nature, 2016. 530(7588): 51-6.
33. Chomont, N., et al., HIV reservoir size and persistence are driven by T cell survival and homeostatic proliferation. Nat Med, 2009. 15(8): 893-900.
34. Buzon, M.J., et al., HIV-1 persistence in CD4+ T cells with stem cell-like properties. Nat Med, 2014. 20(2): 139-42.
35. Coleman, C.M. and L. Wu, HIV interactions with monocytes and dendritic cells: viral latency and reservoirs. Retrovirology, 2009. 6: 51.
36. Thompson, K.A., et al., Brain cell reservoirs of latent virus in presymptomatic HIV-infected individuals. Am J Pathol, 2011. 179(4): 1623-9.
37. Kwon, D.S., et al., DC-SIGN-mediated internalization of HIV is required for trans-enhancement of T cell infection. Immunity, 2002. 16(1): 135-44.
38. Zhang, J. and A.S. Perelson, Contribution of follicular dendritic cells to persistent HIV viremia. J Virol, 2013. 87(14): 7893-901.
39. Eriksson, S., et al., Comparative analysis of measures of viral reservoirs in HIV-1 eradication studies. PLoS Pathog, 2013. 9(2e1003174.
40. Strain, M.C., et al., Highly precise measurement of HIV DNA by droplet digital PCR. PLoS One, 2013. 8(4): e55943.
41. White JA, et al., Measuring the latent reservoir for HIV-1: Quantification bias in near full-length genome sequencing methods. PLoS Pathog. 2022: 18(9): e1010845
42. White JA., et al., Complex decay dynamics of HIV virions, intact and defective proviruses, and 2LTR circles following initiation of antiretroviral therapy. Proc Natl Acad Sci USA, 2022. 8;119(6):e2120326119.

43. Fenton AD., et al., A novel high-throughput microwell outgrowth assay for HIV-infected cells. J Virol, 2024. 19;98(3):e0179823.
44. Bruner KM, Wang Z, et al. A quantitative approach for measuring the reservoir of latent HIV-1 proviruses. Nature, 2019. 566(7742):120–5.
45. Simonetti FR, et al. Intact proviral DNA assay analysis of large cohorts of people with HIV provides a benchmark for the frequency and composition of persistent proviral DNA. Proc Natl Acad Sci, 2020. 117(31):18692–18700.
46. Sannier G, et al. Combined single-cell transcriptional, translational, and genomic profiling reveals HIV-1 reservoir diversity. Cell Rep, 2021. 36(9):109643.
47. Kearney, M.F., et al., Lack of detectable HIV-1 molecular evolution during suppressive antiretroviral therapy. PLoS Pathog, 2014. 10(3):e1004010.
48. Papasavvas E., et al., Intact Human Immunodeficiency Virus (HIV) Reservoir Estimated by the Intact Proviral DNA Assay Correlates With Levels of Total and Integrated DNA in the Blood During Suppressive Antiretroviral Therapy. Clin Infect Dis, 2021. 1;72(3):495-498.
49. Simonetti, F.R., et al., Clonally expanded CD4+ T cells can produce infectious HIV-1 in vivo. Proc Natl Acad Sci U S A, 2016. 113(7):1883-8.
50. Thierry, S., et al., Integrase inhibitor reversal dynamics indicate unintegrated HIV-1 DNA initiate de novo integration. Retrovirology, 2015. 12:24.
51. Chun, T.W., et al., Quantification of latent tissue reservoirs and total body viral load in HIV-1 infection. Nature, 1997. 387(6629):183-8.
52. Siliciano, R.F. and W.C. Greene, HIV latency. Cold Spring Harb Perspect Med, 2011. 1(1): a007096.
53. Murray, A. J., et al., The Latent Reservoir for HIV-1: how immunologic memory and clonal expansion contribute to HIV-1 persistence. J. Immunol, 2016. 197, 407–417.
54. Wagner, T.A., et al., HIV latency. Proliferation of cells with HIV integrated into cancer genes contributes to persistent infection. Science. 2014. 345(6196): 570-3.
55. Wagner TA, et al. An increasing proportion of monotypic HIV-1 DNA sequences during antiretroviral treatment suggests proliferation of HIV-infected cells. J Virol, 2013. 87:1770–8.

56. Maldarelli, F., The role of HIV integration in viral persistence: no more whistling past the proviral graveyard. J Clin Invest, 2016. 126(2): 438-47.
57. Cohn LB, et al. HIV-1 integration landscape during latent and active infection. Cell. 2015;160(3):420–432.
58. Coffin, J.M., et al. The Interactions of Retroviruses and their Hosts, in Retroviruses, 1997: Cold Spring Harbor (NY).
59. Musick A, et al. HIV infected T cells can proliferate in vivo without inducing expression of the integrated provirus. Front Microbiol, 2019. 10:2204.
60. Bailey JR, et al. Residual human immunodeficiency virus type 1 viremia in some patients on antiretroviral therapy is dominated by a small number of invariant clones rarely found in circulating CD4+ T cells. J Virol, 2006. 80:6441–57.
61. Vandergeeten, C., et al., Interleukin-7 promotes HIV persistence during antiretroviral therapy. Blood, 2013. 121(21): 4321-9.
62. Purton, J.F., et al., Antiviral CD4+ memory T cells are IL-15 dependent. J Exp Med, 2007. 204(4): 951-61.
63. Brenchley, J.M., et al., Preferential infection shortens the life span of human immunodeficiency virus-specific CD4+ T cells in vivo. J Virol, 2006. 80(14): p. 6801-9.
64. Wang Z, et al. Expanded cellular clones carrying replication-competent HIV-1 persist, wax, and wane. Proc Natl Acad Sci U S A. 2018;115(11).
65. Halvas EK et al. Nonsuppressible viremia on ART from large cell clones carrying intact proviruses. Boston: Conferences on Retroviruses and Opportunistic Infections; 2019.
66. Geldmacher C, et al. Early depletion of mycobacterium tuberculosis-specific T helper 1 cell responses after HIV-1 infection. J Infect Dis, 2008. 198:1590–8.
67. Liu F, et al. Sequential dysfunction and progressive depletion of Candida albicans-specific CD4 T cell response in HIV-1 infection. PLoS Pathog. 2016. 12:e1005663.
68. Hu H, et al. Distinct gene-expression profiles associated with the susceptibility of pathogen-specific CD4 T cells to HIV-1 infection. Blood, 2013. 121:1136–44.

69. Gomez-Mora E, et al., Preserved immune functionality and high CMV-specific T-cell responses in HIV-infected individuals with poor CD4(+) T-cell immune recovery. Sci Rep, 2017. 7:11711
70. Schroder, A.R., et al., HIV-1 integration in the human genome favors active genes and local hotspots. Cell, 2002. 110(4): p. 521-9.
71. Hayward, W.S., et al., Activation of a cellular onc gene by promoter insertion in ALV-induced lymphoid leukosis. Nature, 1981. 290(5806): 475-80.
72. Jonkers, J. and A. Berns, Retroviral insertional mutagenesis as a strategy to identify cancer genes. Biochim Biophys Acta, 1996. 1287(1): 29-57.
73. Uren, A.G., et al., Retroviral insertional mutagenesis: past, present and future. Oncogene, 2005. 24(52):7656-72.
74. De Ravin, S.S., et al., Enhancers are major targets for murine leukemia virus vector integration. J Virol, 2014. 88(8): 4504-13.
75. Ikeda, T., et al., Recurrent HIV-1 integration at the BACH2 locus in resting CD4+ T cell populations during effective highly active antiretroviral therapy. J Infect Dis, 2007. 195(5): 716-25.
76. Cesana, D., et al., HIV-1-mediated insertional activation of STAT5B and BACH2 trigger viral reservoir in T regulatory cells. Nat Commun. 2017: 8, 498.
77. Igarashi, K., et al., Architecture and dynamics of the transcription factor network that regulates B-to-plasma cell differentiation. J Biochem, 2007. 141(6): 783-9.
78. Muto, A., et al., The transcriptional programme of antibody class switching involves the repressor Bach2. Nature, 2004. 429(6991): 566-71.
79. Sakane-Ishikawa, E., et al., Prognostic significance of BACH2 expression in diffuse large B-cell lymphoma: a study of the Osaka Lymphoma Study Group. J Clin Oncol, 2005. 23(31): 8012-7.
80. Yoshida, C., et al., Bcr-Abl signaling through the PI-3/S6 kinase pathway inhibits nuclear translocation of the transcription factor Bach2, which represses the antiapoptotic factor heme oxygenase-1. Blood, 2007. 109(3): 1211-9.
81. Tsukumo, S., et al., Bach2 maintains T cells in a naive state by suppressing effector memory-related genes. Proc Natl Acad Sci U S A, 2013. 110(26): 10735-40.

82. Roychoudhuri, R., et al., BACH2 represses effector programs to stabilize T(reg)-mediated immune homeostasis. Nature, 2013. 498(7455): 506-10.
83. Kim, E.H., et al., Bach2 regulates homeostasis of Foxp3+ regulatory T cells and protects against fatal lung disease in mice. J Immunol, 2014. 192(3): 985-95.
84. Roychoudhuri, R., et al., The transcription factor BACH2 promotes tumor immunosuppression. J Clin Invest, 2016. 126(2): 599-604.
85. Chen, H., et al., Acute promyelocytic leukemia with a STAT5b-RARalpha fusion transcript defined by array-CGH, FISH, and RT-PCR. Cancer Genet, 2012. 205(6): 327-31.
86. Burchill, M.A., et al., Linked T cell receptor and cytokine signaling govern the development of the regulatory T cell repertoire. Immunity, 2008. 28(1): 112-21.
87. Malek, T.R., et al., CD4 regulatory T cells prevent lethal autoimmunity in IL-2Rbeta-deficient mice. Implications for the nonredundant function of IL-2. Immunity, 2002. 17(2): 167-78.
88. Burchill, M.A., et al., Interleukin-2 receptor signaling in regulatory T cell development and homeostasis. Immunol Lett, 2007. 114(1): 1-8.
89. Jenks, J.A., et al., Differentiating the roles of STAT5B and STAT5A in human CD4+ T cells. Clin Immunol, 2013. 148(2): 227-36.
90. Vogtenhuber, C., et al., Constitutively active Stat5b in CD4+ T cells inhibits graft-versus-host disease lethality associated with increased regulatory T-cell potency and decreased T effector cell responses. Blood. 2010: 116(3): 466-74.
91. Moreno-Fernandez, M.E., et al. Homeostasis and function of regulatory T cells in HIV/SIV infection. J Virol, 2012.86(19):10262-9.
92. Macatangay, B.J. and C.R. Rinaldo, Regulatory T cells in HIV immunotherapy. HIV Ther, 2010. 4(6): 639-647.
93. Song, Y., Tr1 Cells as a Key Regulator for Maintaining Immune Homeostasis in Transplantation. Front. Immunol, 2021. 12:671579.
94. Chevalier, M.F. and L. Weiss, The split personality of regulatory T cells in HIV infection. Blood, 2013. 121(1): 29-37.
95. Jenabian, M.A., et al., Distinct tryptophan catabolism and Th17/Treg balance in HIV progressors and elite controllers. PLoS One, 2013. 8(10): e78146.

96. Chevalier, M.F., et al., The Th17/Treg ratio, IL-1RA and sCD14 levels in primary HIV infection predict the T-cell activation set point in the absence of systemic microbial translocation. PLoS Pathog, 2013. 9(6): e1003453.
97. Tran, T.A., et al., Resting regulatory CD4 T cells: a site of HIV persistence in patients on long-term effective antiretroviral therapy. PLoS One, 2008. 3(10): e3305.
98. Gabrilovich, D. I. et al. The terminology issue for myeloid-derived suppressor cells. Cancer Res, 2007. 67; 425.
99. Ziegler-Heitbrock, L., et al. Nomenclature of monocytes and dendritic cells in blood. Blood, 2010. 116:e74– e80.
100. Yoon. B.R., et al., Functional phenotype of synovial monocytes modulating inflammatory T-cell responses in rheumatoid arthritis (RA). PloS One, 2014. 9: e109775.
101. Bain, C.C., et al., Resident and pro-inflammatory macrophages in the colon represent alternative context-dependent fates of the same Ly6Chi mono- cyte precursors. Mucosal Immunol, 2013. 6:498–510.
102. Waschbisch, A., et al., Pivotal role for CD16+ monocytes in immune surveillance of the central nerv- ous system. J Immunol. 2016. 196:1558–1567.
103. Morell, M., et al., Myeloid populations in systemic autoimmune diseases. Clin Rev Allergy Immunol, 2017. 53:198–218.
104. Amoruso, A., et al., Relation among anti-rheumatic drug therapy, CD14(+)CD16(+) blood monocytes and disease activity markers (DAS28 and US7 scores) in rheumatoid arthritis: a pilot study. Pharmacol Res, 2016. 107:308–314.
105. Steinman and Banchereau, Taking dendritic cells into medicine. Nature, 2007. 449; 419-426.
106. Rescigno, M., Di Sabatino, A. Dendritic cells in intestinal homeostasis and disease. J Clin Invest, 2009. 119:2441–2450.
107. Banchereau and Steinman, Dendritic cells and the control of immunity. Nature, 1998. 392; 245-252107.
108. Schwartz, R.H., et al., T-cell clonal anergy. Cold Spring Harb Symp Quant Biol, 1989. 54(Pt 2):605–610.

109. Dhodapkar, M.V. et al., Antigen-specific inhibition of effector T cell function in humans after injection of immature dendritic cells. J Exp Med, 2001. 193:233–238.
110. Manches et al., Dendritic cells in progression and pathology of HIV infection. Trends Immunol, 2014. 35;114-122.
111. Gregori, S., et al., Differentiation of type 1 T regulatory cells (Tr1) by tolerogenic DC-10 requires the IL-10-dependent ILT4/HLA-G pathway. Blood, 2010. 116:935–944.
112. Saraiva M, et al., Interleukin-10 production by Th1 cells requires interleukin-12-induced STAT4 transcription factor and ERK MAP kinase activation by high antigen dose. Immunity, 2009. 31:209–19.
113. Mosser, D.M., Zhang, X., Interleukin-10: new perspectives on an old cytokine. Immunol Rev, 2008. 226:205–218.
114. Zheng, Z., et al. Induction of T cell anergy by the treatment with IL-10-treated dendritic cells. Comp Immunol Microbiol Infect Dis, 2004. 27:93–103.
115. Donnelly, R.P., et al., The interleukin-10 signal transduction pathway and regulation of gene expression in mononuclear phagocytes. J Interferon Cytokine Res, 1999. 19:563–573.
116. Moreau, P., et al., IL-10 selectively induces HLA-G expression in human trophoblasts and monocytes. Int Immunol, 1999. 11:803–811.
117. Vlad, G., et al., Interleukin-10 induces the upregulation of the inhibitory receptor ILT4 in monocytes from HIV positive individuals. Hum Immunol, 2003. 64:483–489.
118. Lee, T.S., Chau LY: Heme oxygenase-1 mediates the anti-inflammatory effect of interleukin-10 in mice. Nat Med, 2002. 8:240–246.
119. Velten, F.W., et al., A gene signature of inhibitory MHC receptors identifies a BDCA3(+) subset of IL-10-induced dendritic cells with reduced allostimulatory capacity in vitro. Eur J Immunol, 2004. 34:2800–2811.
120. Ancuta, P., et al., CD14+CD16++ cells derived in vitro from peripheral blood monocytes exhibit phenotypic and functional dendritic cell-like characteristics. Eur J Immunol, 2000. 30:1872–1883.

121. Comi M., et al., Coexpression of CD163 and CD141 identifies human circulating IL-10-producing dendritic cells (DC-10). Cell Mol Immunol, 2020. 17: 95–107.
122. Rizzo, R., et al., HLA-G Molecules in Autoimmune Diseases and Infections. Front Immunol, 2014. 5:592.
123. Amodio, G., et al., HLA-G expressing DC-10 and CD4(+) T cells accumulate in human decidua during pregnancy. Hum Immunol,2013. 74: 406–11.
124. Locafaro, G., et al., HLA-G expression on blasts and tolerogenic cells in patients affected by acute myeloid leukemia. J Immunol Res, 2014. 2014:636292.
125. Xu, D.P., et al. Elevation of HLA-G- expressing DC-10 cells in patients with gastric cancer. Hum Immunol, 2016. 77:800–4.
126. Amodio, G., et al. Altered Frequency and Phenotype of HLA-G-Expressing DC-10 in Type 1 Diabetes Patients at Onset and in Subjects at Risk to Develop the Disease. Front Immunol, 2021. 1;12:750162.
127. Pena-Cruz, V., et al., HIV-1 replicates and persists in vaginal epithelial dendritic cells. J Clini Invest, 2018. 128:3439–44.
128. Kijewski, S.D. et Gummuluru, S., A mechanistic overview of dendritic cell-mediated HIV-1 trans infection: the story so far. Future Virol, 2015. 10:257–69.
129. Barron, M.A., et al., Influence of plasma viremia on defects in number and immunophenotype of blood dendritic cell subsets in human immunodeficiency virus 1-infected individuals. J Infect Dis, 2003. 187:26–37.
130. Sabado, R.L., et al., Evidence of dysregulation of dendritic cells in primary HIV infection. Blood. 2010. 116:3839–52.
131. Diao, Y., et al., Low CD1c + myeloid dendritic cell counts correlated with a high risk of rapid disease progression during early HIV-1 infection. BMC Infect Dis, 2015. 15:342.
132. Huang, J., et al., Leukocyte immunoglobulin-like receptors maintain unique antigen-presenting properties of circulating myeloid dendritic cells in HIV-1-infected elite controllers. J Virol, 2010. 84:9463–71.
133. Manches, O., et al., Activation of the noncanonical NF-kappaB pathway by HIV controls a dendritic cell immunoregulatory phenotype. Proc Natl Acad Sci USA, 2012. 109:14122–7.

134. Gayo, E., et al. A reproducibility-based computational framework identifies an inducible, enhanced antiviral state in dendritic cells from HIV-1 elite controllers. Genome Biol, 2018. 19:10.
135. Granelli-Piperno A., et al., HIV-1-infected monocyte-derived dendritic cells do not undergo maturation but can elicit IL-10 production and T cell regulation. Proc Natl Acad Sci U S A, 2004. 18;101(20):7669-74.
136. Cabello. A., et al., HAART induces the expression of HLA-G on peripheral monocytes in HIV-1 infected individuals. Hum Immunol, 2003. 64(11):1045-9.
137. Svanberg, C., et al. HIV-1 induction of tolerogenic dendritic cells is mediated by cellular interaction with suppressive T cells. Front. Immunol, 2022. 13:790276.
138. Bruner, K.M., et al., A quantitative approach for measuring the reservoir of latent HIV-1 proviruses. Nature, 2019: 566, 120–125.
139. Firouzi, S. et al. Development and validation of a new high-throughput method to investigate the clonality of HTLV-1-infected cells based on provirus integration sites. Genome medicine, 2014. 6, 46-46.
140. Spinozzi, G. et al. VISPA2: a scalable pipeline for high-throughput identification and annotation of vector integration sites. BMC Bioinformatics. 2017. 18, 520.
141. Naji, A. et al. CD3+CD4low and CD3+CD8low are induced by HLA-G: novel human peripheral blood suppressor T-cell subsets involved in transplant acceptance. Blood, 2013. 110, 3936-3948.
142. LeMaoult, J., et al., HLA-G1-expressing antigen-presenting cells induce immunosuppressive CD4+ T cells. Proc Natl Acad Sci U S A, 2004. 101, 7064-7069.
143. Lila, N., et al., Soluble HLA-G protein secreted by allo-specific CD4+ T cells suppresses the allo-proliferative response: a CD4+ T cell regulatory mechanism. Proc Natl Acad Sci USA, 2001. 98: 12150-12155.
144. Amodio G., et al. HLA-G expression levels influence the tolerogenic activity of human DC-10. Haematologica, 2015. 100, 548-557.
145. Comi M., et al. Interleukin-10-Producing DC-10 Is a Unique Tool to Promote Tolerance Via Antigen-Specific T Regulatory Type 1 Cells. Frontiers in immunolog, 2018. 9; 682.

146. Malnati M., et al., Activating Killer Immunoglobulin Receptors and HLA-C: a successful combination providing HIV-1 control. Sci Rep, 2017. 7, 42470.
147. Biffi, A., et al., Lentiviral vector common integration sites in preclinical models and a clinical trial reflect a benign integration bias and not oncogenic selection. Blood, 2011. 117, 5332-5339.
148. Tran, T.A., et al., Resting regulatory CD4 T cells: a site of HIV persistence in patients on long-term effective antiretroviral therapy. PLoS One, 2008. 3(10): p. e3305.
149. Mellors et al., Insertional activation of STAT3 and LCK by HIV-1 proviruses in T cell lymphomas. Sci. Adv, 2021. 7: eabi8795
150. Coffin, M., et al., Clones of infected cells arise early in HIV-infected individuals. JCI Insight, 2019. 4(12):e128432.
151. Fraietta JA, et al. Disruption of TET2 promotes the therapeutic efficacy of CD19-targeted T cells. Nature, 2018. 558(7709):307–312
152. Wu, V.H., et al., Assessment of HIV-1 integration in tissues and subsets across infection stages. JCI Insight, 2020. 5(20):e139783.
153. Simonetti, F.R., et al., Antigen-driven clonal selection shapes the persistence of HIV-1–infected CD4+ T cells in vivo. J Clin Inves,. 2021. 131(3):e145254.
154. Picelli, S. et al. Smart-seq2 for sensitive full-length transcriptome profiling in single cells. Nature methods, 2013. 10, 1096-1098.
155. Picelli, S. Et Al. Full-Length Rna-Seq From Single Cells Using Smart-Seq2.
156. Muccini C., et al., People with four-class drug-resistant HIV-1 may have low levels of intact DNA. AIDS, 2025. 39(4):p 475-476.
157. Ananworanich, J. et al. Impact of multi-targeted antiretroviral treatment on gut T cell depletion and HIV reservoir seeding during acute HIV infection.
158. Moldt B., et al., Evaluation of HIV-1 reservoir size and broadly neutralizing antibody susceptibility in acute antiretroviral therapy-treated individuals. AIDS, 2022. 36(2):205-214.
159. Falcinelli SD, Kilpatrick KW, Read J, Murtagh R, Allard B, Ghofrani S, et al. Longitudinal dynamics of intact HIV proviral DNA and outgrowth virus frequencies in a cohort of indivi- duals receiving antiretroviral therapy. J Infect Dis 2020; 224:92–100.

160. Barbehenn, A., et al., Rapid biphasic decay of intact and defective HIV DNA reservoir during acute treated HIV disease. *Nat Commun*, 2024. 15: 9966.
161. Bruner KM., et al., Defective proviruses rapidly accumulate during acute HIV-1 infection. Nat Med, 2016. 22:1043–9.
162. Sáez-Cirión A., et al., Post-treatment HIV-1 controllers with long-term virological remission after the interruption of early initiated antiretroviral therapy, ANRS VISCONTI Study. PLoS Pathog 2013; 9:e10032111.
163. Lodi S., et al., Immunovirologic control 24 months after interruption of antiretroviral therapy initiated close to HIV seroconversion. Arch Intern Med,2012. 172:1252–1255.
164. Martin GE., et al., Posttreatment control or treated controllers? Viral remission in treated and untreated primary HIV infection. AIDS, 2017. 31:477–484.
165. The SPARTAC Trial Investigators. Short-course antiretroviral therapy in primary HIV infection. New Engl J Med, 2013. 368:207–217.
166. Kiepiela P., et al., Dominant influence of HLA-B in mediating the potential co-evolution of HIV and HLA. Nature, 2004. 432:769–775.
167. Goulder PJR., et al., HIV and HLA class I: an evolving relationship. Immunity, 2012. 37:426–440
168. Migueles SA., et al., HLA B∗5701 is highly associated with restriction of virus replication in a subgroup of HIV-infected long term nonprogressors. Proc Natl Acad Sci U S A, 2000. 97:2709–2714.
169. Cao K., et al., Analysis of the frequencies of HLA-A, B, and C alleles and haplotypes in the five major ethnic groups of the United States reveals high levels of diversity in these loci and contrasting distribution patterns in these populations. Hum. Immunol, 2001. 62:1009–1030.
170. Chen H., et al., CD4+ T cells from elite controllers resist HIV-1 infection by selective upregulation of p21. J. Clin. Invest, 2011. 121:1549–1560.
171. Chen H., et al., Differential neutralization of human immunodeficiency virus (HIV) replication in autologous CD4 T cells by HIV-specific cytotoxic T lymphocytes. J. Virol, 2009. 83:3138–3149.
172. Miura T., et al., HLA-B57/B*5801 human immunodeficiency virus type 1 elite controllers select for rare gag variants associated with reduced viral replication

capacity and strong cytotoxic T-lymphocyte recognition. J. Virol, 2009. 83:2743–2755.

173.Gao F., et al., Influence of KIR and NK Cell Reconstitution in the Outcomes of Hematopoietic Stem Cell Transplantation. Front Immunol, 2020. 2;11:2022.

174.Rizzo S., et al., Role of KIR Receptor in NK Regulation during Viral Infections. Immuno,2021. 1(3), 305-331.

